# Enhanced Interferon Signaling Pathway in Oral Cancer Revealed by Quantitative Proteome Analysis of Microdissected Specimens Using $^{16}O/^{18}O$ Labeling and Integrated Two-dimensional LC-ESI-MALDI Tandem MS*[S]

**Lang-Ming Chi‡§, Chien-Wei Lee‡, Kai-Ping Chang¶, Sheng-Po Hao¶, Hang-Mao Lee‡, Ying Liang‡, Chuen Hsueh‡‖, Chia-Jung Yu‡**, I-Neng Lee‡, Yin-Ju Chang‡, Shih-Ying Lee‡, Yuan-Ming Yeh‡‡, Yu-Sun Chang‡ ‡‡, Kun-Yi Chien‡**§§, and Jau-Song Yu‡**¶¶**

**Oral squamous cell carcinoma (OSCC) remains one of the most common cancers worldwide, and the mortality rate of this disease has increased in recent years. No molecular markers are available to assist with the early detection and therapeutic evaluation of OSCC; thus, identification of differentially expressed proteins may assist with the detection of potential disease markers and shed light on the molecular mechanisms of OSCC pathogenesis. We performed a multidimensional $^{16}O/^{18}O$ proteomics analysis using an integrated ESI-ion trap and MALDI-TOF/TOF MS system and a computational data analysis pipeline to identify proteins that are differentially expressed in microdissected OSCC tumor cells relative to adjacent non-tumor epithelia. We identified 1233 unique proteins in microdissected oral squamous epithelia obtained from three pairs of OSCC specimens with a false discovery rate of <3%. Among these, 977 proteins were quantified between tumor and non-tumor cells. Our data revealed 80 dysregulated proteins (53 up-regulated and 27 down-regulated) when a 2.5-fold change was used as the threshold. Immunohistochemical staining and Western blot analyses were performed to confirm the overexpression of 12 up-regulated proteins in OSCC tissues. When the biological roles of 80 differentially expressed proteins were assessed via MetaCore™ analysis, the interferon (IFN) signaling pathway emerged as one of the most significantly altered pathways in OSCC. As many as 20% (10 of 53) of the up-regulated proteins belonged to the IFN-stimulated gene (ISG) family, including ubiquitin cross-reactive protein (UCRP)/ISG15. Using head-and-neck cancer tissue microarrays, we determined that UCRP is overexpressed in the majority of cheek and tongue cancers and in several cases of larynx cancer. In addition, we found that IFN-$\beta$ stimulates UCRP expression in oral cancer cells and enhances their motility *in vitro*. Our findings shed new light on OSCC pathogenesis and provide a basis for the future development of novel biomarkers.** ***Molecular & Cellular Proteomics 8:1453–1474, 2009.***

Oral cancer is one of the most common cancers worldwide. In Taiwan, it remains the sixth most prevalent cancer overall and the fourth most common cancer to afflict males. Over the past 2 decades, the overall incidence and morbidity rates of patients with oral cancer have increased continuously. Epidemiological studies show that ~50–70% of patients who undergo surgery for oral cancer die within 5 years (1–6). This poor prognosis predominantly reflects late stage presentation, secondary cancer occurrence, local recurrence, and metastasis (7) as well as the lack of suitable markers for cancer detection. Therefore, there is an urgent need to identify proteins that are dysregulated in patients with oral cancer. Such proteins would serve as a valuable resource to find markers for the early diagnosis and disease monitoring of patients with oral cancer.

Oral cancer, a subtype of head-and-neck squamous cell carcinoma (HNSCC),[1] can form at various locations within the

From the ‡Molecular Medicine Research Center, **Department of Biochemistry and Molecular Biology, and ‡‡Graduate Institute of Biomedical Sciences, College of Medicine, Chang Gung University and Departments of §Medical Research and Development, ¶Otolaryngology-Head and Neck Surgery, and ‖Pathology, Chang Gung Memorial Hospital, Tao-Yuan 333, Taiwan

Received, October 6, 2008, and in revised form, March 9, 2009

Published, MCP Papers in Press, March 18, 2009, DOI 10.1074/mcp.M800460-MCP200

[1] The abbreviations used are: HNSCC, head-and-neck squamous cell carcinoma; IT, ion trap; IFN, interferon; IHC, immunohistochemical; LCM, laser capture microdissection; OSCC, oral squamous cell carcinoma; SCX, strong cation exchange; UCRP, ubiquitin cross-reactive protein; ISCP, ISG15-conjugated protein; 2D, two-dimensional; DMEM, Dulbecco's modified Eagle's medium; SFM, serum-free medium; MudPIT, multidimensional protein identification technology; XML, extensible markup language; SERPH, serpin H1; HSP47, heat-shock protein of 47 kDa; STAT1, signal transducer and activator of transcription 1; TYPH, thymidine phosphorylase; FLN,

oral cavity, including the lips, tongue, buccal surfaces, gingiva, palate, floor of mouth, and oropharynx. Tongue and buccal cancers are the most common and most serious types of oral squamous cell carcinoma (OSCC) especially in southeast Asia (2, 8). Alcohol abuse, smoking, and betel nut chewing are the main risk factors for OSCC. Genome-wide approaches have revealed many epigenetic and genetic alterations in patients with OSCC, including several biochemical pathways (9–11). However, these studies have provided little information regarding alterations in the protein profiles of patients with OSCC. Recently state-of-the-art proteomics technologies have revealed alterations in protein abundance, posttranslational modification and turnover, and spatial and temporal distribution within tumor specimens. Using proteomics approaches, aberrantly expressed proteins have been identified in body fluids (12–14), frozen or paraffin-embedded tissues (15–18), and cultured cell lines (19–22). The fold changes in protein expression in samples from healthy and cancerous states as well as the roles of each protein in disease progression must be determined to identify potential candidates for biomarkers and therapeutic targets.

Blood samples are often used in clinical studies because they are less invasive and more convenient than other types of bodily samples and can be analyzed using automatic and high throughput techniques. Unfortunately the extremely dynamic range of protein concentrations in serum and plasma impedes the direct discovery of potential biomarkers (23, 24). Proteins can be released into the blood from diseased tissues during cell death or via secretory pathways. To counteract this problem, serum and plasma biomarkers are sometimes identified by analyzing differential protein expression in tumors and adjacent normal tissues (25).

Like many other types of solid tumors, OSCCs often contain heterogeneous cell populations. Laser capture microdissection (LCM) is a common technique used to dissect a particular tumor cell type from heterogeneous cell populations, thereby reducing the tissue complexity and facilitating the discovery of tumor-associated molecules in small samples (9, 26–28). Several laboratories have studied differential protein expression in microdissected tissue specimens from patients with head-and-neck cancer in efforts to discover novel tumor markers (15, 17, 29–31). However, the semiquantitative approaches used in these studies may have limited the number of potential markers identified as well as the reliability of the protein quantification. To minimize technical variations and improve the reliability of protein quantification, a variety of sophisticated stable isotope labeling techniques have been developed for MS-based proteomics analysis, including chemical (32, 33), metabolic (34, 35), and enzymatic (36–38) labeling techniques. Improvements in the quality and accuracy of quantitative proteomics analysis via such stable isotope labeling strategies have facilitated the discovery of potential tumor markers in malignancies such as OSCC/HNSCC (16, 39, 40).

Here we describe a strategy consisting of LCM, $^{18}O$ labeling, two-dimensional (2D) LC separation and an integrated ESI-MS/MS and MALDI-TOF/TOF MS (ESI-MALDI tandem MS) system. This strategy was used to identify differentially expressed proteins in OSCC cells microdissected from oral cancer tissue biopsies. A computational data analysis pipeline was also developed to calculate the relative abundances of $^{16}O$- and $^{18}O$-labeled peptides (similar to that described in a previous report (26)) and to assist with multidimensional protein identification and quantification. Using three pairs of OSCC specimens, we identified 1233 unique proteins with a false discovery rate less than 3%. Of these, we quantified 977 non-redundant proteins in which 80 proteins displayed ≥2.5-fold changes in expression in microdissected tumor cells *versus* non-tumor cells. We validated these results in 12 selected targets via immunohistochemical staining and Western blot analysis of OSCC tissues. Our findings reveal that the interferon (IFN) signaling pathway is significantly altered in OSCC lesions.

## EXPERIMENTAL PROCEDURES

### *Clinical Specimens*

Three pairs of specimens of surgically resected primary OSCC lesions and adjacent non-tumorous tissues were obtained from three male patients for use in LCM. The specimens were immediately embedded in O.C.T. (Optimal Cutting Temperature) compound (Tissue-Tek® O.C.T., Sakura Finetek) and stored at −70 °C until use. Before conducting the LCM experiments, the tissue sections were stained with hematoxylin/eosin and evaluated by a pathologist. All of the tissue samples were collected from patients who had signed informed consent forms prior to participation in the study, which was approved by the Institutional Review Board of Chang Gung Memorial Hospital at Lin-Ko, Taiwan. Clinicopathological data from paired specimens used in LCM, immunohistochemical (IHC) staining, and Western blot analyses are summarized in supplemental Table S1. Head-and-neck tumor tissue microarrays (BC34011, head-and-neck squamous cell carcinoma tissue arrays) containing 60 head-and-neck squamous cell carcinoma tissues and three normal gingival tissues were obtained from US Biomax, Inc. (Rockville, MD).

### *Cell Culture*

The OC3 cell line (a derivative of the OSCC cell line derived from the cheek of an areca chewing/non-smoking male patient (41)) was

filamin; FSCN1, fascin; SODM, mitochondrial superoxide dismutase; GBP, interferon-induced guanylate-binding protein; ANXA3, annexin A3; CAH2, carbonic anhydrase II; T, tumor; N, non-tumor; GO, Gene Ontology; TENA, tenascin; FINC, fibronectin; GP, glycoprotein; ISG, IFN-stimulated gene; ISGylation, posttranslational modification with ISG15; CK, cytokeratin; LDHA, L-lactate dehydrogenase A chain; EPIPL, epiplakin; EVPL, envoplakin; PEPL, periplakin; 6PGD, 6-phosphogluconate dehydrogenase; SERA, D-3-phosphoglycerate dehydrogenase; SYWC, tryptophanyl-tRNA synthetase; AMPL, cytosol aminopeptidase; PML, probable transcription factor PML; ACTN1, alpha-actinin-1; BIGH3, transforming growth factor beta-induced 68 kDa protein; IFM1, interferon-induced transmembrane protein-1; K1C, type I cytokeratin; MX1, interferon-induced GTP-binding protein Mx1; NDRG1, *N*-myc downstream regulated gene 1; TSP1; thrombospondin-1.

kindly provided by Dr. Kuo-Wei Chang (School of Dentistry, National Yang-Ming University, Taiwan). The SCC4 tongue squamous cell carcinoma line was derived from a 55-year-old male (ATCC number CRL-1624), and the OEC-M1 oral epidermal carcinoma cell line was derived from the gingiva of a Chinese patient (42). The OC3 cells were cultured in a medium composed of DMEM (Invitrogen) containing 10% fetal calf serum and Keratinocyte-SFM (Invitrogen) (at a 1:2 ratio), and the SCC4 and OEC-M1 cells were grown in RPMI 1640 medium containing 10% fetal bovine serum, 25 mM HEPES, and antibiotics at 37 °C in 5% $CO_2$.

*LCM and Protein Extraction for LC-MS/MS Analysis*

In preparation for LCM, 8-$\mu$m cryosections were mounted onto membrane slides. The slides were fixed with 70% ethanol for 30 s, washed with 25% ethanol for 45 s, placed in Mayer's hematoxylin solution for 30 s, rinsed with 75% ethanol, dehydrated once in 95% ethanol, cleared twice in 100% xylene for 30 s each, and thoroughly air-dried. Laser capture microdissection was performed using the Veritas Laser Capture Microdissection and Laser Cutting Systems (Arcturus, Mountain View, CA). Briefly the tissue surrounding the selected area was cut using a UV laser, and the internal areas were irradiated via soft IR laser pulses to dissociate the cut sections from the membrane slides. Several selected areas were then adhered to a CapSure LCM Cap (Arcturus) and immediately transferred to a 0.5-ml microcentrifuge tube for protein extraction. All captured cells were dissolved in 50–100 $\mu$l of lysis buffer (7 M urea, 2 M thiourea, 1% Triton X-100, and 50 mM Tris-HCl, pH 8.0) by vortexing at room temperature for 30 min, briefly sonicating the samples in an ice bath, and centrifuging at 20,000 $\times$ *g* for 10 min to remove insoluble debris. The concentrations of the protein extracts were measured via a modified Bradford assay (Bio-Rad), and the proteins were further examined by SDS-PAGE and silver staining as described previously (43, 44). We extracted ~60–80 $\mu$g of protein from $1.0 \times 10^6$–$1.5 \times 10^6$ microdissected cells.

*Postdigestion $^{18}O$ Labeling*

The extracted proteins were diluted 6-fold in 100 mM ammonium bicarbonate and digested twice with trypsin (1:50, w/w) at room temperature for 12 h each. Detergent and salts were removed via sequential strong cation exchange (Luna SCX, 5 $\mu$m, Phenomenex) and $C_{18}$ reverse phase (LiChroprep RP18, 5–20 $\mu$m, Merck) microtip columns. After drying the peptides under a vacuum, the samples were added to $^{16}O$ or $^{18}O$ labeling solutions containing 1 $\mu$g of trypsin, 20 mM $CaCl_2$, and 50 mM Tris-HCl, pH 8.0, in $H_2{}^{16}O$ or $H_2{}^{18}O$ (Sigma-Aldrich). Trypsin-catalyzed $^{16}O$ or $^{18}O$ labeling was performed overnight at 37 °C. Trypsin was inactivated by incubation in a boiling water bath for 15 min and acidification with formic acid to a final concentration of 3% (similar to that described in a previous report (26)).

*2D LC Separation*

Equally mixed $^{16}O$- and $^{18}O$-labeled peptides (derived from 20 $\mu$g of proteins/sample) were injected into a BioBasic SCX column (5 $\mu$m, 2.1 $\times$ 150 mm, ThermoElectron) on an HPLC system (Waters Breeze HPLC instrument) and eluted on a 60-min ammonium chloride gradient in the presence of 25% acetonitrile, pH 3.0 (adjusted using formic acid). The effluents were pooled into 20 fractions, dried, and redissolved in 3% acetonitrile containing 0.01% TFA. Each fraction was loaded into a NanoEase $C_{18}$ trapping column (5 $\mu$m, 0.18 $\times$ 23.5 mm, Symmetry300™) and separated on a 60-min acetonitrile gradient (ranging from 3 to 40%) on a capillary RP18 column (3.5 $\mu$m, 0.15 $\times$ 150 mm, Symmetry300, Waters). In preparation for integrated ESI and MALDI MS analysis, the effluent was split with a Nano Y-connector (Upchurch Scientific, Oak Harbor, WA) that diverted the flow by a ratio of 1:3 to the ESI source and to a 384-well target plate attached to a ProBot spotting robot (LC Packings/Dionex) with a 10-s collection time. The samples were mixed with $\alpha$-cyano-4-hydroxycinnamic acid matrix (2 mg/ml in 80% ACN and 0.1% TFA) containing 3 fmol of internal standards in the 384-well target plate as previously described (45). The samples were then analyzed using a MALDI-TOF/TOF (Ultraflex TOF/TOF, Bruker Daltonics, Bremen, Germany) MS system under the management of FlexControl (version 2.2) and WarpLC (version 1.0) software (Bruker Daltonics).

*LC-ESI-MALDI Tandem MS Analysis*

ESI-IT data acquisition was performed using the Esquire3000plus (Bruker Daltonics) with EsquireControl 5.2 software. Peptide fragment spectra were acquired from one MS scan followed by six MS/MS scans of the most abundant parent ions. Each precursor ion was analyzed twice and then excluded in the following minute. Automatic and intelligent MALDI-TOF/TOF data acquisition was performed using WarpLC software (Bruker Daltonics) with an LC-ESI-MALDI work flow, which performs a low redundancy parent ion selection by excluding peptides already identified by ESI-MS/MS analysis. Compounds spanning more than 60% of the MALDI-TOF MS spectra in a 384-well plate were considered background signals and were excluded from the parent precursor list. In each spectrum, eight of the most abundant peaks with signal-to-noise ratios higher than 30 were selected as parent precursors and were used in tandem MS assays in laser-induced fragmentation technique (LIFT™) mode with FlexControl 2.2 software.

*MS Data Processing and Database Search*

The emerging spectra identified via ESI-MS/MS and MALDI-TOF/TOF MS were analyzed using DataAnalysis 3.4 and FlexAnalysis 2.4 peak picking software (Bruker Daltonics), respectively, and used in searches of the Swiss-Prot_51.6 database (selected for *Homo sapiens*, 15,720 entries) assuming trypsin as the digestion enzyme. The MASCOT search engine (version 2.2.03, Matrix Science, London, UK) was used with one missing cleavage site; MS tolerance values of 2.5 and 0.8 Da for ESI-IT and WARP-ESI-MALDI data sets, respectively; MS/MS tolerance values of 0.6 Da for both data sets; and variable modifications of peptide including methionine oxidation and double $^{18}O$ labeling of the carboxyl terminus. Protein identification was performed using probability-based Mowse (molecular weight search) scores ($p < 0.05$) and the MudPIT algorithm of the MASCOT search engine. Information derived from MS spectra and database searches was exported into Microsoft Excel and XML file formats, respectively, for further $^{16}O/^{18}O$ quantification analysis. The false discovery rate of protein identification was determined by searching the MASCOT-generated decoy database (using the same parameters described above) and was adjusted to false discovery rate <3% for each experiment. The resulting list of distinguishable proteins was generated by excluding identifications obtained solely from shared peptides and by including proteins containing at least one distinct peptide with a score higher than the identity threshold in MASCOT (but that was not shared with other identified proteins). Protein quantification was performed using the resulting distinguishable protein data set.

*Protein Quantification Pipeline*

The quantification pipeline is shown in Fig. 1*B*. This pipeline involves three main steps.

*Step 1: Localization of Identified Peptides on the MALDI Plate*—From the exported MASCOT search results (XML files), each rank 1 peptide with an ion score >15 was analyzed to locate the well

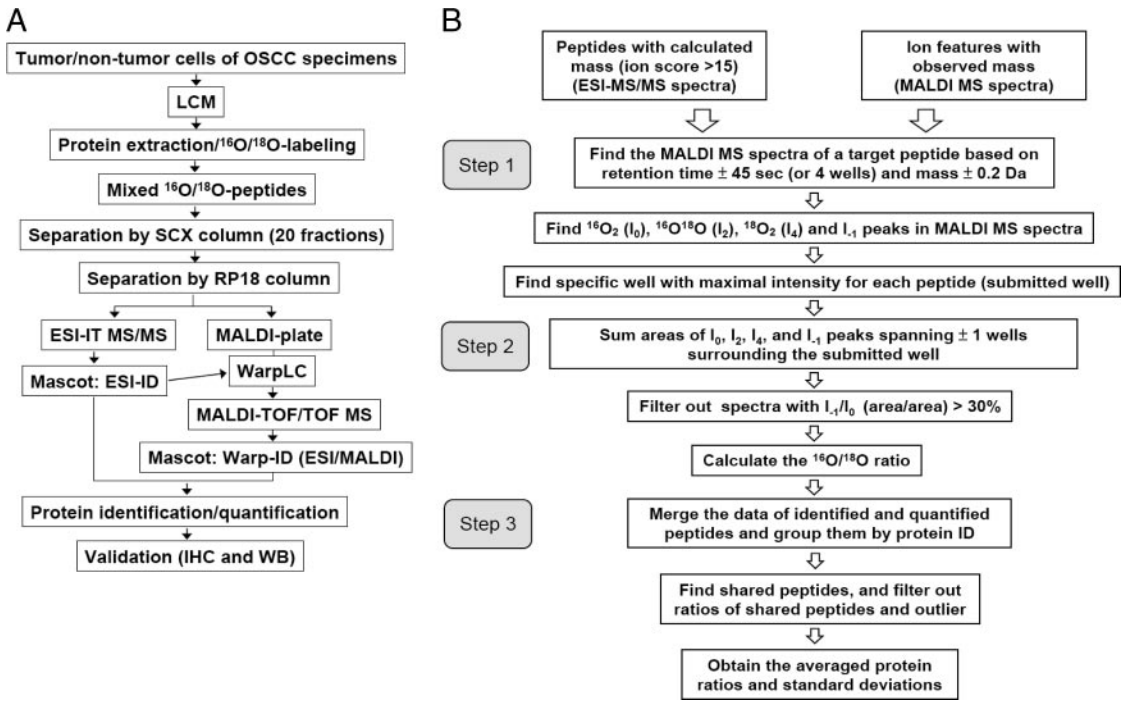


FIG. 1. **The $^{16}O/^{18}O$ quantitative proteomics strategy for analyzing microdissected OSCC tissue specimens.** *A*, the $^{16}O/^{18}O$ labeling process and integration of the ESI and MALDI tandem MS techniques. WarpLC refers to a software platform developed by Bruker Daltonics for assistance with the generation and integration of ESI and MALDI data. *WB*, Western blot analysis. *B*, a schematic illustration of the computational pipeline for $^{16}O/^{18}O$ quantitative proteomics analysis. Briefly the pipeline started from exporting all MASCOT search results generated in ESI and MALDI tandem MS measurements. And then the MALDI MS spectrum of target ion corresponding to a particular peptide query was found based on the calculated mass (±0.2 Da) and retention time (±45 s or 4 wells) of the identified peptide. The relative abundance of paired peptides was then calculated using the peak area of the paired $^{16}O/^{18}O$ signals ($I_0$, $I_2$, and $I_4$ ions) considering the theoretical isotopic distribution of the chemical elements in a particular peptide. Finally the abundance ratios of peptides determined in all LC-MS runs were put together to calculate the relative abundance of their corresponding proteins. See "Experimental Procedures" for details.

corresponding to the MALDI MS spectra. The correspondent wells for peptides identified in the MALDI-TOF/TOF analysis were defined as the wells where TOF/TOF measurements were performed. The correspondent wells of peptides detected via ESI were determined from the ESI chromatographic retention times. In general, the retention time of each identified peptide, minus the delay time for sample collection on the MALDI plate (chromatographic offset time), was divided by 10 (because of the 10-s collection time per well) to translate the retention time into the well information. The well with the maximum ion intensity for a particular compound was identified by scanning forward and backward in 4-well regions surrounding the correspondent well and submitted as the apex of a particular ion chromatography (the submitted well).

*Step 2: Peak Pairing, Relative Abundance Calculation, and Summation of Three Consecutive Well Fractions*—The *m/z* values and intensities of the paired monoisotopic peaks ($I_0$, $I_2$, and $I_4$ for the $^{16}O_2$-, $^{16}O/^{18}O$-, and $^{18}O_2$-labeled peptides, respectively) were determined for each located well. Only paired peaks containing all isotopic peaks ($I_0$, $I_2$, and $I_4$) were selected for further analysis. To minimize interference from overlapping peaks in the peptide quantification, the paired peaks with front neighbor ions ($I_{-1}$ or $I_0 - 1$) displaying more than 30% of the intensity of $I_0$ were filtered out. Finally, we determined the sum of the peak areas spanning ±1 well surrounding the submitted well for a particular ion displaying a 0.2-Da mass tolerance of the calculated mass of the identified peptide. The relative abundance of the identified peptide was then calculated based on the theoretical isotopic distribution, which was computed using the Isotopic Pattern Calculator as described previously (26).

*Step 3: Protein Grouping and Abundance Evaluation*—Peptides that had been identified and quantified via multidimensional fractionations were then combined and grouped by Swiss-Prot entry name. To improve the reliability of protein identification and quantification, shared and carboxyl-terminal peptides were filtered out during quantitative analysis. A Dixon's test (using a critical *Q* value corresponding to a 95% confidence level) was applied to remove the outlier ratios of peptides. Protein abundance ratios and standard deviations were then calculated. For proteins containing only one or two quantified distinct peptides, the protein ratios and their associated deviations were directly averaged without further consideration. To account for errors in sample preparation, the protein abundance ratios for each experiment were readjusted via global median normalization in which the individual protein ratios were divided by the median value of all quantified protein ratios in each experiment.

### *Immunohistochemical Staining*

IHC staining analyses were performed using an automatic immunohistochemical staining device according to the manufacturer's instructions (Bond™, Vision Biosystems, Mount Waverley, Victoria, Australia) and as reported previously (46). Consecutive sections (5 $\mu$m thick) of formalin-fixed, paraffin-embedded specimens from 10 OSCC patients were stained with various antibodies using the Envision kit (Dako Corp., Carpinteria, CA). Immunohistochemical analyses were performed using specific antibodies against ubiquitin cross-reactive protein (UCRP) (a rabbit polyclonal antibody; kindly donated by Dr. Leroy F. Liu, University of Medicine and Dentistry of New Jersey,

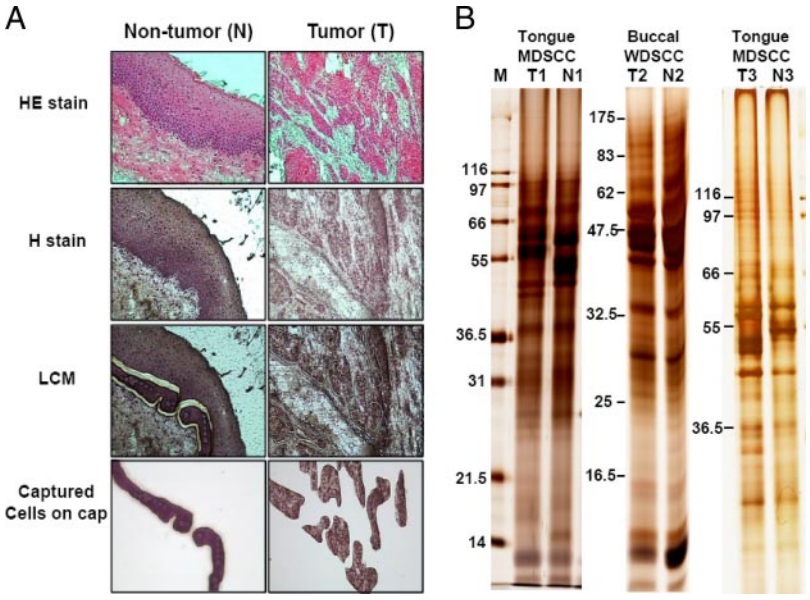


FIG. 2. **LCM-assisted dissection of OSCC epithelial cells and SDS-PAGE analysis of proteins extracted from microdissected cells.** *A*, tissue cryosections were fixed and stained with hematoxylin/eosin (*HE*) in preparation for pathological analysis. Tissue specimens were stained with hematoxylin (*H*) for use in LCM experiments. *B*, protein samples (5 $\mu$g) extracted from three paired microdissected tumor (*T*) and adjacent non-tumor (*N*) epithelial cells were resolved by SDS-PAGE and examined via silver staining. The region within the oral cavity and the differentiation status of each OSCC specimen used for LCM analysis and protein extraction are indicated at the *top* of the figure. *MDSCC*, moderately differentiated squamous cell carcinoma; *WDSCC*, well differentiated squamous cell carcinoma. *Lane M*, molecular weight markers in kDa.

Robert Wood Johnson Medical School, Piscataway, NJ; 1:250), serpin H1/heat-shock protein of 47 kDa (SERPH/HSP47; Santa Cruz Biotechnology sc5293; 1:100), transforming growth factor $\beta$-induced 68-kDa protein (BIGH3; homemade anti-rabbit polyclonal antibody; 1:300), signal transducer and activator of transcription 1 (STAT1-$\alpha/\beta$; BD Biosciences; 1:100), thymidine phosphorylase (TYPH; Lab Vision clone PGF.44C; 1:500), filamin B (FLNB; Chemicon ab9276; 1:20), filamin A (FLNA; Chemicon mab1680; 1:250), fascin (FSCN1; Santa Cruz Biotechnology sc21743; 1:300), mitochondrial superoxide dismutase (SODM; Santa Cruz Biotechnology sc30080; 1:200), interferon-induced guanylate-binding protein 1 (GBP1; Santa Cruz Biotechnology sc53857; 1:300), annexin A3 (ANXA3; Abcam; 1:200), carbonic anhydrase II (CAH2; Chemicon ab1828; 1:200), and IFN-$\beta$ (R&D Systems mab814; 1:150). The intensities and percentages of positive staining of the target cells were determined by pathologists (Ying Liang and Chuen Hsueh) and used for quantitative scoring. Staining intensity was graded using four scores with 0 representing a negative stain and 1, 2, and 3 indicating weak, moderate, and strong staining, respectively. Scores were then multiplied by the percentage of positively stained cells to obtain the final protein expression score. The final expression scores were classified into four groups, including negative staining (scores of 0), weak staining (scores of 10–70), moderate staining (scores of 80–170), and strong staining (scores $\geq$180).

### *Western Blot Analysis*

Cell extracts were prepared as described previously (47), and protein concentrations were determined using the Bradford protein assay reagent (Bio-Rad). Samples (30 $\mu$g of protein/lane) were separated by 8 or 15% SDS-PAGE, transferred to PVDF membranes (Millipore Corp.), and probed using primary antibodies against the candidates of interest as described previously (43, 44). For analyzing IFN-stimulated gene expression by Western blot, the OC3 or SCC4 cells were washed twice with PBS and then incubated in fresh medium with or without IFN-$\beta$ (PeproTech Inc.) for 24 h.

### *Functional Annotation and Network Analysis*

Differentially expressed proteins detected via quantitative proteomics analysis were functionally classified according to Gene Ontology biological process using ProteinCenter™ (Proxeon Biosystems, Odense, Denmark). Network analyses of protein candidates and the ratios of their expression in tumor and non-tumor cells (obtained from five independent experiments) were performed using the MetaCore™ analytical suite version 4.7 (GeneGo, Inc., St. Joseph, MI) and compared using $p$ values $<0.01$ as statistical metrics. The statistical significance of the identified networks was based on $p$ values, which are defined as the probability that a given number of proteins from the input list will match a certain number of gene nodes in the network.

### *Cell Proliferation Assay*

Cell proliferation was evaluated using a 3-(4,5-dimethylthiazol-2-yl)-2,5-diphenyltetrazolium bromide assay as described in supplemental Fig. S5.

### *Transwell Migration Assay*

Cell migration was assayed in 24-well Transwell chambers (using an 8-$\mu$m-pore filter) (Costar, Corning Inc., NY). The OC3 cells were suspended in 300 $\mu$l of serum-free DMEM and Keratinocyte-SFM in a 1:2 ratio and were treated with or without IFN-$\beta$ (20 units/ml) (PeproTech Inc.). The cells were then inserted into the upper chamber, while the lower chambers were filled with 600 $\mu$l of serum-free DMEM and Keratinocyte-SFM in a 1:2 ratio containing 10 $\mu$g/ml fibronectin (Sigma). After a 6-h incubation at 37 °C, the chambers were gently washed twice with PBS, fixed in methanol, and stained

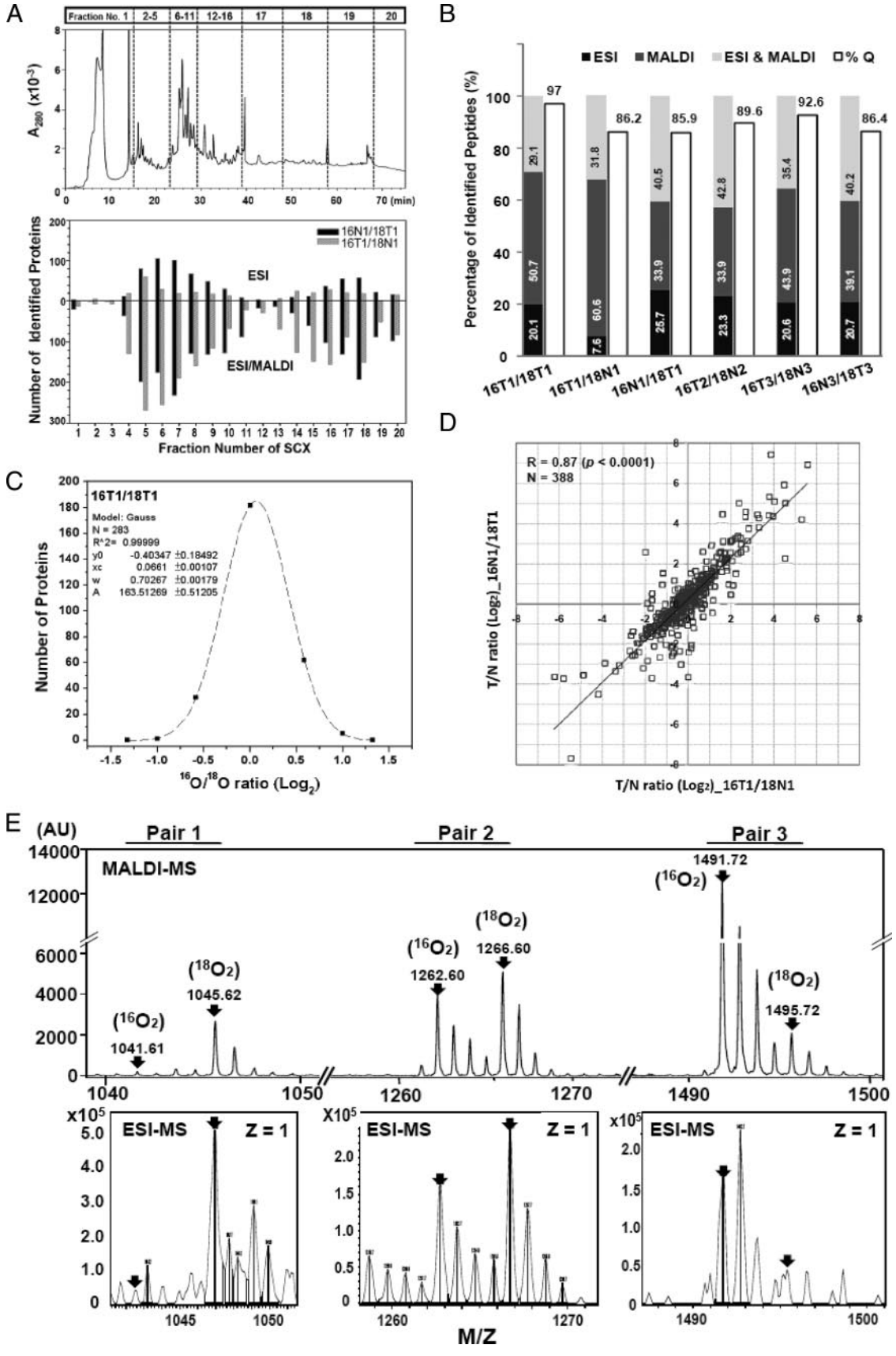
A
Fraction No. 1
2-5
6-11
12-16
17
18
19
20
A280 (x10-3)
70 (min)
16N1/18T1
16T1/18N1
ESI
ESI/MALDI
Number of Identified Proteins
Fraction Number of SCX
B
ESI
MALDI
ESI & MALDI
% Q
Percentage of Identified Peptides (%)
97
86.2
85.9
89.6
92.6
86.4
16T1/18T1
16T1/18N1
16N1/18T1
16T2/18N2
16T3/18N3
16N3/18T3
C
16T1/18T1
Model: Gauss
N = 283
R^2= 0.99999
y0 -0.40347 ±0.18492
xc 0.0661 ±0.00107
w 0.70267 ±0.00179
A 163.51269 ±0.51205
Number of Proteins
16O/18O ratio (Log2)
D
R = 0.87 (p < 0.0001)
N = 388
T/N ratio (Log2)_16N1/18T1
T/N ratio (Log2)_16T1/18N1
E
(AU)
Pair 1
Pair 2
Pair 3
MALDI-MS
(16O2)
1041.61
(18O2)
1045.62
(16O2)
1262.60
(18O2)
1266.60
(16O2)
1491.72
(18O2)
1495.72
ESI-MS
Z = 1
M/Z

with Giemsa. The numbers of cells that traversed the filter to the lower chamber were counted at a 400× magnification in six fields per filter using NIH Image J software (version 1.4g, National Institutes of Health, Bethesda, MD). Results were expressed as means of cell number ± S.D. Statistical analysis was performed using two-sided, unpaired Student's *t* test with *p* values less than 0.05 considered significant.

## RESULTS

*Experimental Design and Sample Preparation*—We designed an $^{18}O$ labeling-based protein identification and quantification approach with two integrated MS systems to identify dysregulated proteins in OSCC tumor cells and adjacent non-tumor epithelia (Fig. 1*A*) in which a computational pipeline for integration of the ESI and MALDI tandem MS data was developed (Fig. 1*B*). The epithelial cells of the primary OSCCs and their adjacent non-tumorous tissues were dissected by LCM and used for protein extraction. Fig. 2*A* shows representative images of tumor and non-tumor epithelia sections before and after LCM. The quality and quantity of proteins extracted from the three pairs of microdissected samples (T1/N1, T2/N2, and T3/N3) were examined by SDS-PAGE followed by silver staining (Fig. 2*B*). The results revealed that although the T2/N2 pair seems similar, a difference in protein bands ranging from 36.5 to 66 kDa could be detected in the tumor and non-tumor parts of T1/N1 and T3/N3 pairs. For example, when compared with T1, N1 shows an additional prominent band around 50 kDa and the lack of a band around 45 kDa. In addition, the protein profiles of the three pairs are not similar to each other, indicating the heterogeneous nature of the patient sample pairs. Equal amounts of extracted proteins were then trypsin-digested and labeled in $^{16}O$ or $^{18}O$ buffer solution. Two pairs of samples containing sufficient amounts of extracted proteins were swap-labeled (16T1/18N1 *versus* 16N1/18T1 and 16T3/18N3 *versus* 16N3/18T3), and another sample containing a lower amount of extracted proteins was analyzed via $^{16}O$ labeling of *tumor* cells and $^{18}O$ labeling of *non-tumor* cells (16T2/18N2) only.

*Protein Identification by Multidimensional Separation and Integrated ESI-IT-MS/MS and MALDI-TOF/TOF MS Analysis*—The first dimension contained equally mixed $^{16}O/^{18}O$-labeled peptides separated by SCX chromatography into 20 fractions (Fig. 3*A*, *upper panel*). These fractions were then subjected to simultaneous second dimensional on-line LC-ESI and off-line LC-MALDI analyses. Protein identification was performed using WarpLC software. In each SCX fraction of sample 1, the number of proteins identified using the MASCOT algorithm (by ESI alone or by integrated ESI-MALDI analysis) are summarized in Fig. 3*A*, *lower panel*. The number of unique proteins identified using the integrated ESI-MALDI strategy increased by ~45–100% in each SCX fraction as compared with the number of proteins identified using ESI-IT alone. Approximately 33–60% of the total unique peptides identified in ESI-MALDI mode (in six independent experiments) could only be determined by MALDI-TOF/TOF analysis (Fig. 3*B*). The benefit of using MALDI-TOF MS spectra to obtain quantitative information is that this technique generates less complex spectra and higher impurity tolerance than the ESI MS system (48–50). In addition, the femtomolar sensitivity and the 1:10 dynamic range of quantification can be achieved by $^{18}O$ labeling in MALDI-TOF MS measurement (51). Therefore, the abundance of peptides identified using integrated ESI and MALDI MS systems was calculated using MALDI-TOF MS spectra, thereby generating more accurate mass measurements and higher resolution than is possible with conventional ESI-IT MS.

*Quantification of ESI-MALDI-identified Peptides by the MALDI-TOF MS Spectra*—The reliability of MS-based quantification, especially for $^{16}O/^{18}O$-labeled peptides, depends highly on the resolution and accuracy of the MS spectrum (52). As mentioned earlier, the spectra generated in MALDI-TOF MS are of sufficient quality for quantifying $^{16}O/^{18}O$-labeled peptides in contrast to the spectra generated in traditional ESI-IT MS (52). However, the integrated ESI-MALDI MS system can be challenging with regard to the alignment of ion features generated from the ESI and MALDI MS peptide measurements (using MALDI MS spectra). To address this issue, we developed a computational pipeline to determine

FIG. 3. **Performance of the integrated ESI and MALDI tandem MS system.** *A*, comparison of proteins identified via ESI and ESI/MALDI tandem MS. The $^{16}O/^{18}O$-peptides were separated by SCX chromatography, pooled into 20 fractions, and subjected to LC-ESI/MALDI MS/MS analysis. A representative SCX chromatogram of 16N1/18T1 is shown in the *upper panel*. The numbers of unique proteins identified in 16N1/16T1 (*black bar*) and 16T1/18N1 (*gray bar*) using the ESI and integrated ESI/MALDI MS systems are shown in the *lower panel*. *B*, complimentary peptide identification using the integrated ESI/MALDI platform. The percentage of total unique peptides identified by ESI, MALDI, and the two MS systems (in six independent experiments) is shown *inside* the *bar graph*. More than 85% of the identified unique peptides were quantified using MALDI MS spectra (*blank bars* refer to percent of quantified peptides (Q)). *C*, the accuracy of each $^{16}O/^{18}O$ labeling experiment was evaluated using an equally mixed $^{16}O/^{18}O$-sample prepared from a specific tumor specimen (16T1/18T1). The $\log_2$ ratio distributions of the 283 quantified proteins were fitted with a Gaussian function using OriginPro 7.5 software (OrignLab Corp., Northampton, MA). The mean (xc) and the two standard deviation (*w*) values were calculated from the formula: $y = y_0 + (A/\sqrt{(\pi w^2/2)})e(-2((x - xc)/w)^2)$. *D*, the reliability of protein quantification was examined in paired tumor and non-tumor samples that had been reciprocally labeled with $^{16}O$ or $^{18}O$ (16N1/18T1 and 16T1/18N1). The linear correlation of quantification in the swapped samples was demonstrated using a correlation coefficient of 0.87. "*N*" refers to the number of proteins simultaneously identified and quantified in the swapped samples. *E*, representative MS spectra obtained in MALDI and ESI MS systems demonstrate differences in the resolution of each MS system. Reduced (*left panel*), unaffected (*middle panel*), and increased (*right panel*) $^{16}O$ ion features (as compared with $^{18}O$-labeled features) are indicated. *AU*, arbitrary units.

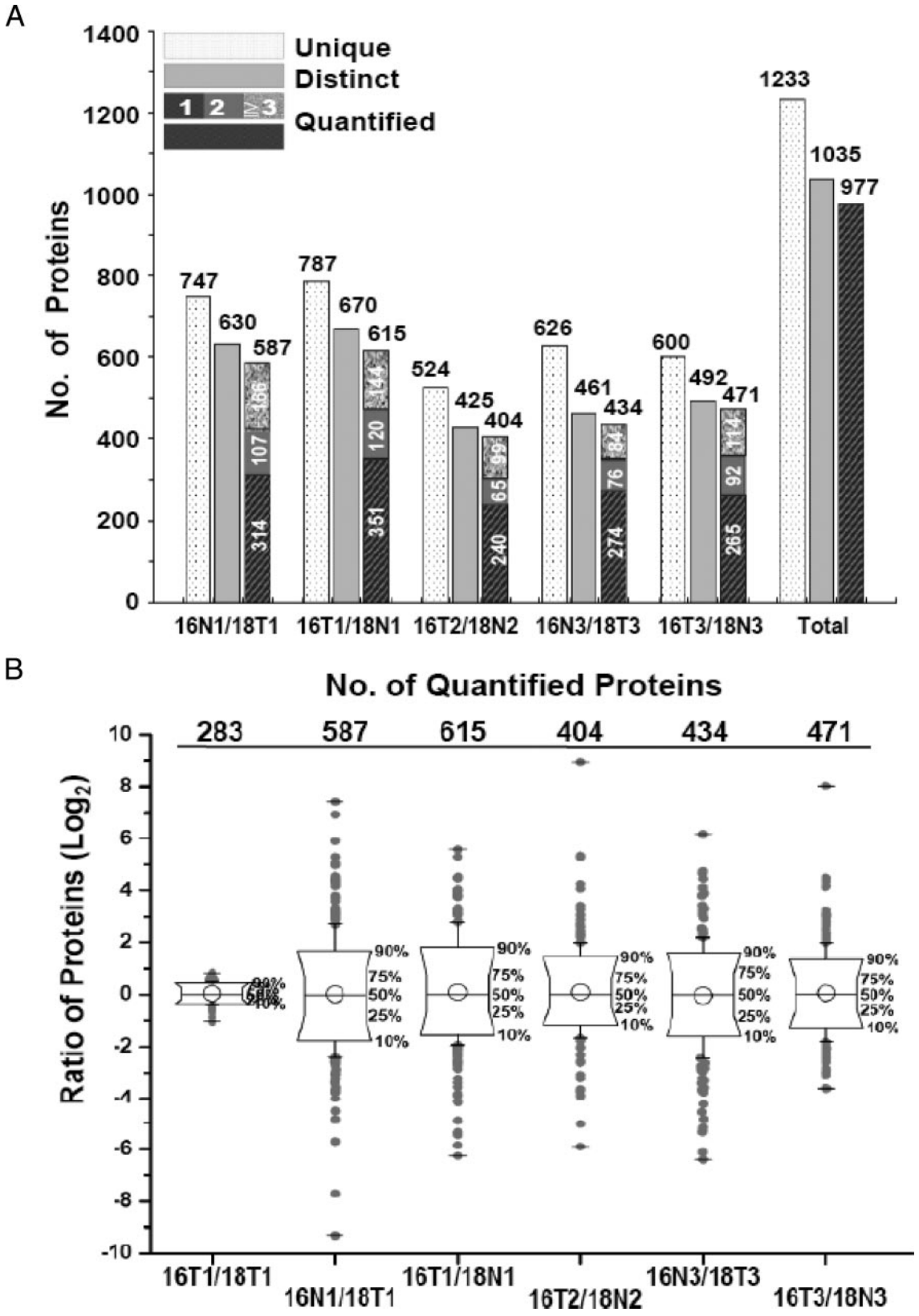


FIG. 4. **Identification and quantification of proteins in microdissected oral epithelia using the $^{16}O$ and $^{18}O$ labeling and integrated ESI/MALDI tandem MS techniques.** *A*, number of unique (*dotted bars*) and distinct (*gray bars*) proteins and number of proteins (*stacked* and *slashed bars*) quantified. The number of proteins quantified using one, two, or ≥3 peptides in each experiment is indicated *inside* each *bar*.

the matched MALDI-TOF MS spectra of all identified peptides (Fig. 1*B*). The performance of this alignment-and-quantification pipeline was first evaluated by calculating the percentage of the quantified peptides. As shown in Fig. 3*B* (*blank bar*), more than 85% of the identified peptides (with ion scores >15) could be quantified. The accuracy of protein quantification was then evaluated using equally mixed model samples of 16T1/18T1 (a mixture containing equal amounts of $^{16}O$- and $^{18}O$-labeled peptides prepared from the microdissected tumor cells of sample 1). In this experiment, 283 proteins were quantified, and their log-transformed protein ratios could be fitted into a Gaussian distribution with a mean of 0.0661 (about 1.05 in original scale) and two standard deviations of 0.70267 (Fig. 3*C*). Wherein ~95% of the proteins displayed fold changes in the range of −0.64 to 0.77 (mean ± 2S.D.; equal to 0.64–1.7 in original scale). The correlation between protein identification and quantification was then assessed using a swap-labeled sample set (16T1/18N1 and 16N1/18T1) in which 388 proteins were simultaneously identified and quantified in both samples with a linear correlation coefficient of ~0.87 (Fig. 3*D*). The representative MALDI-TOF MS spectra and the corresponding ESI spectra obtained via LC-ESI/MALDI MS analysis of a specific SCX-separated fraction from 16T1/18N1 are shown in Fig. 3*E*. These findings illustrate the different resolutions of the two MS systems while simultaneously indicating the change in $^{16}O$ ion features relative to the $^{18}O$-labeled features. In summary, these results demonstrate the feasibility of our integrated ESI-MALDI strategy for use in $^{16}O/^{18}O$-labeled protein identification and quantification. This method was subsequently used to identify differentially expressed proteins among the three pairs of microdissected OSCC samples.

*Identification of Differentially Expressed Proteins in OSCC Tissue Specimens*—Using MudPIT scoring (the MASCOT algorithm), 747, 787, 524, 626, and 600 unique proteins were identified within 16N1/18T1, 16T1/18N1 (sample 1), 16T2/18N2 (sample 2), 16N3/18T3, and 16T3/18N3 (sample 3), respectively, with corresponding false determination rates of 2.72, 1.06, 2.19, 1.39, and 1.39 (Fig. 4*A*). With regard to the reliability of protein identification, proteins identified by peptides with scores higher than the identity threshold that were not shared with other proteins were selected as distinguishable proteins and included in further quantification analysis. In all, 572, 593, 386, 439, and 466 proteins (of the 615, 648, 406, 466, and 486 distinguishable proteins, respectively) were quantified (Fig. 4*A*). In summary, 1233, 1035, and 977 unique, distinguishable, and quantified proteins, respectively, were identified from the three pairs of OSCC specimens (as determined by five independent experiments). Detailed identification and quantification information for the 977 quantified proteins is available in supplemental Tables S2-1 (protein list) and S2-2 (peptide list). The MS/MS spectra and the correspondent fragment assignments of the single distinct peptide-based protein identifications are summarized in supplemental Fig. S1. Distributions of the normalized protein ratios are displayed as box plot diagrams in Fig. 4*B*. The 95% distribution of protein ratios determined in the equally mixed model sample (16T1/18T1) fall within the 0.64–1.7 range (Fig. 3*C*); thus, proteins displaying an average T/N ratio higher than 2 or lower than 0.5 were selected for further consideration. Among these proteins, those displaying an average fold change of ≥2.5 in tumor *versus* non-tumor parts in at least three experiments were chosen as potential candidates for future analysis. Considering the limited identification rate of shotgun proteomics as well as the inherent heterogeneity of OSCC, distinguishable proteins that were detected in two of the five experiments but that displayed average fold changes greater than 5 or less than 0.2 were also selected as potential candidates. After analysis of the 977 quantified proteins, 53 up-regulated and 27 down-regulated candidates were identified and were classified by biological process category using Gene Ontology (GO) (Tables I and II). Details regarding the identification and quantification of these 80 proteins are shown in supplemental Table S3. Among the 53 up-regulated proteins, 71.7% were involved in cell proliferation (8 of 53; 15.1%), defense (8 of 53; 15.1%), communication (8 of 53; 15.1%), cell motility (7 of 53; 13.2%), or cell organization/biogenesis (7 of 53; 13.2%), consistent with the well known biological properties of tumor cells. The majority of the 27 down-regulated candidates were involved in metabolism (11 of 27; 40.7%) and epidermal development (6 of 27; 22.2%). A literature search revealed that nine of the 53 up-regulated proteins (K1C16, FSCN1, TYPH, TENA, SERPH, SODM, FINC, TSP1, and NDRG1) are known to be overexpressed in OSCC. In addition, 18 of the 53 up-regulated proteins and four of the 27 down-regulated proteins are known to be dysregulated in other cancer types (Table I and references cited therein).

*Validation of Candidates by Immunohistochemical Staining and Western Blotting*—Commercially available antibodies were used in Western blot analyses to examine the expression of eight up-regulated candidates in three paired oral biopsies. The results revealed increased expression of seven proteins (UCRP, fascin, GBP1, ANXA3, HSP47, STAT1, and FLNA) in two of the three tumor biopsies (Fig. 5*A*). We then examined the expression of the eight up-regulated candidates and four additional proteins (thymidine phosphorylase, mitochondrial superoxide dismutase, filamin B, and carbonic anhydrase II) in

The number of total proteins identified is shown at the *top* of each *bar*. *B*, the ratio distributions of proteins quantified in each experiment are presented as box plot diagrams. The mean value of all ratios (○), the percentages of ratio data points, and the minimum and maximum data points (−) are indicated.

TABLE I
*Up-regulated candidates in OSCC*

| GO[a] | Swiss-Prot | | Gene name | T/N ratio[b] | | | | | | | Cancer association[c] (detection method[c]) (Ref.) | | Possible regulation |
|---|---|---|---|---|---|---|---|---|---|---|---|---|---|
| | ID_HUMAN | Code | | 16N1 | 16T1 | 16T2 | 16N3 | 16T3 | Mean | Freq. | OSCC | Other cancers | |
| Cell proliferation | | | | | | | | | | | | | |
| 1 | SYWC | P23381 | *WARS* | 20.50 | 13.53 | 40.60 | 25.57 | 17.38 | 23.52 | 5/5 | | | ISG-ISCP |
| 2 | BIGH3 | Q15582 | *TGFBI* | 21.48 | 2.98 | 2.31 | 3.60 | 3.89 | 6.85 | 5/5 | | Colon (86, 87), pancreas (88) | |
| 3 | K1C16 | P08779 | *KRT16* | 60.25 | 22.40 | 0.48 | 26.77 | 22.69 | 26.52 | 4/5 | (P, IHC) (15) | | |
| 4 | K2C6A | P02538 | *KRT6A* | 39.40 | 13.90 | 0.51 | 2.85 | 1.32 | 11.60 | 3/5 | | | |
| 5 | FSCN1 | Q16658 | *FSCN1* | 8.51 | 3.93 | 1.04 | 1.93 | 2.45 | 3.57 | 3/5 | (IHC, TMA) (89, 90) | Esophagus (91, 92), colon (93), kidney (94), breast (95), lung (96), ovary (97) | |
| 6 | ITA6 | P23229 | *ITGA6* | 1.36 | 3.97 | ND | 3.01 | 2.54 | 2.72 | 3/4 | | | |
| 7 | IFM1 | P13164 | *IFITM1* | ND | ND | 3.02 | 4.90 | 2.59 | 3.50 | 3/3 | | | ISG |
| 8 | K2C6E | P48668 | *KRT6C* | 22.12 | NQ | 1.14 | 9.88 | NQ | 11.04 | 2/3 | | Lung (98) | |
| Cell organization and biogenesis | | | | | | | | | | | | | |
| 9 | STAT1 | P42224 | *STAT1* | 7.70 | 5.53 | 3.94 | 8.37 | 4.54 | 6.02 | 5/5 | | Stomach (99) | ISG-ISCP |
| 10 | TYPH | P19971 | *TYMP* | 9.45 | 5.48 | 2.30 | 5.13 | 5.10 | 5.49 | 5/5 | (G, P, IHC) (100–102) | Pancreas (103), breast (104), nasopharynx (105) | ISG |
| 11 | FLNB | O75369 | *FLNB* | 2.77 | 4.68 | 2.24 | 5.70 | 3.52 | 3.78 | 5/5 | | | ISCP |
| 12 | FLNA | P21333 | *FLNA* | 4.53 | 3.50 | 2.17 | 2.32 | 2.08 | 2.92 | 5/5 | | | ISCP |
| 13 | P4HA1 | P13674 | *P4HA1* | ND | 15.80 | ND | 9.32 | 18.06 | 14.39 | 3/3 | | Breast (106), stomach (107) | |
| 14 | LIMA1 | Q9UHB6 | *LIMA1* | ND | 6.98 | ND | 3.10 | 2.71 | 4.26 | 3/3 | | | |
| 15 | LRC59 | Q96AG4 | *LRRC59* | 3.00 | 2.44 | ND | 4.06 | ND | 3.17 | 3/3 | | | |
| Defense | | | | | | | | | | | | | |
| 16 | UCRP | P05161 | *ISG15* | 33.38 | 16.40 | 38.99 | 9.26 | 8.71 | 21.35 | 5/5 | | Bladder (82), breast (83) | ISG |
| 17 | MX1 | P20591 | *MX1* | 8.66 | 6.87 | 5.41 | 3.80 | 4.43 | 5.83 | 5/5 | | | ISG-ISCP |
| 18 | HLAG | P17693 | *HLA-G* | NQ | ND | 3.07 | 5.35 | 6.34 | 4.92 | 3/3 | | Stomach (108) | |
| 19 | PGAM1 | P18669 | *PGAM1* | 2.69 | 2.36 | 2.56 | ND | ND | 2.53 | 3/3 | | | |
| 20 | GBP1 | P32455 | *GBP1* | NQ | NQ | NQ | 13.88 | 20.39 | 17.13 | 2/2 | | | ISG-ISCP |
| 21 | HB2G | P01911 | *HLA-DRB2* | ND | ND | ND | 7.64 | 9.47 | 8.56 | 2/2 | | | |
| 22 | GBP2 | P32456 | *GBP2* | ND | 8.37 | NQ | NQ | 4.16 | 6.27 | 2/2 | | | ISG |
| 23 | 2DRA | P01903 | *HLA-DRA* | 2.64 | ND | 7.37 | ND | ND | 5.01 | 2/2 | | | |
| Cell communication | | | | | | | | | | | | | |
| 24 | TENA | P24821 | *TNC* | 31.49 | 23.29 | 1.57 | 14.71 | 260.92 | 66.40 | 4/5 | (IHC) (109, 110) | | |
| 25 | EPIPL | P58107 | *EPPK1* | 17.82 | 39.40 | 1.23 | 4.33 | 2.76 | 13.11 | 4/5 | | | ISCP |
| 26 | FIBB | P02675 | *FGB* | 21.19 | 9.40 | 2.75 | 2.06 | 1.69 | 7.42 | 4/5 | | | |
| 27 | CKAP4 | Q07065 | *CKAP4* | 5.74 | 3.18 | 1.44 | 2.73 | 2.18 | 3.05 | 4/5 | | | |
| 28 | LDHA | P00338 | *LDHA* | 2.94 | 2.98 | 1.69 | 3.82 | 2.16 | 2.72 | 4/5 | | | ISCP |
| 29 | FIBA | P02671 | *FGA* | 13.13 | 7.12 | 0.47 | 1.32 | 2.03 | 4.82 | 3/5 | | | |
| 30 | LAMB3 | Q13751 | *LAMB3* | 19.94 | 15.55 | ND | ND | ND | 17.74 | 2/2 | | | |
| 31 | ANXA3 | P12429 | *ANXA3* | 19.66 | 6.39 | ND | ND | NQ | 13.02 | 2/2 | | | ISCP |
| Regulation of biological process | | | | | | | | | | | | | |
| 32 | K1C17 | Q04695 | *KRT17* | 170.90 | 14.56 | 3.64 | 72.45 | 8.23 | 53.96 | 5/5 | | Basal cell (111) | |
| 33 | SERPH | P50454 | *SERPINH1* | 13.73 | 9.91 | 2.93 | 10.72 | 8.34 | 9.13 | 5/5 | (G, IHC) (112) | Pancreas (113, 114) | ISCP |
| 34 | PML | P29590 | *PML* | 8.50 | 3.07 | ND | 2.87 | ND | 4.81 | 3/5 | | Thyroid (115) | ISG-ISCP |
| 35 | GRP78 | P11021 | *HSPA5* | 3.83 | 2.87 | 1.30 | 3.14 | 1.93 | 2.61 | 3/5 | | Stomach (116), esophagus (117) | |
| 36 | SODM | P04179 | *SOD2* | 0.86 | ND | 9.62 | 2.93 | 2.42 | 3.96 | 3/4 | (P, IHC) (22) | Head and neck (118), esophagus (119) | |
| Cell motility | | | | | | | | | | | | | |
| 37 | S10A2 | P29034 | *S100A2* | 4.49 | 3.43 | 1.11 | 3.16 | 4.13 | 3.26 | 4/5 | | Pancreas (120), esophagus (121), bladder (122) | |
| 38 | FINC | P02751 | *FN1* | 23.45 | 6.40 | ND | 5.86 | 3.81 | 9.88 | 4/4 | (G, IHC) (123) | Ovary (124), breast (125), head and neck (126), larynx (127) | |

TABLE I—*continued*

| GO[a] | Swiss-Prot | | Gene name | T/N ratio[b] | | | | | | Cancer association[c] (detection method[c]) (Ref.) | | Possible regulation |
|---|---|---|---|---|---|---|---|---|---|---|---|---|
| | ID_HUMAN | Code | | 16N1 | 16T1 | 16T2 | 16N3 | 16T3 | Mean | Freq. | OSCC | Other cancers | |
| 39 | ITB4 | P16144 | *ITGB4* | 5.54 | 3.19 | 2.85 | ND | 2.36 | 3.48 | 4/4 | | | |
| 40 | ACTN1 | P12814 | *ACTN1* | 8.74 | 4.13 | 1.43 | 4.27 | 1.20 | 3.95 | 3/5 | | | ISCP |
| 41 | TPM4 | P67936 | *TPM4* | 7.94 | NQ | NQ | 4.52 | 3.54 | 5.34 | 3/3 | | | |
| 42 | TSP1 | P07996 | *THBS1* | 121.61 | 47.79 | ND | ND | ND | 84.70 | 2/2 | (IHC) (128, 129) | Head and neck (130), cervix (131), prostate (132), colon (133), stomach (134) | |
| 43 | LAMC2 | Q13753 | *LAMC2* | 4.69 | 23.03 | ND | ND | ND | 13.86 | 2/2 | | | |
| Development | | | | | | | | | | | | | |
| 44 | NDRG1 | Q92597 | *NDRG1* | 5.84 | 5.50 | 0.52 | 3.00 | 3.94 | 3.76 | 4/5 | (G, WB, IHC) (135) | Liver (136, 137), colon (138) | |
| 45 | COCA1 | Q99715 | *COL12A1* | 31.45 | 5.09 | ND | 16.69 | 2.16 | 13.85 | 4/4 | | | |
| 46 | APOL2 | Q9BQE5 | *APOL2* | ND | 8.38 | 4.64 | 17.35 | 2.47 | 8.21 | 4/4 | | | |
| 47 | K1C14 | P02533 | *KRT14* | 18.85 | 9.90 | 0.51 | 1.77 | 5.72 | 7.35 | 3/5 | | HNSCC (139) | |
| 48 | CAH2 | P00918 | *CA2* | ND | ND | 3.27 | NQ | 7.70 | 5.49 | 2/2 | | | |
| Metabolism | | | | | | | | | | | | | |
| 49 | OXRP | Q9Y4L1 | *HYOU1* | 3.98 | 2.71 | ND | 2.53 | 2.87 | 3.02 | 4/4 | | | |
| 50 | AMPL | P28838 | *LAP3* | ND | 1.45 | 6.54 | 4.06 | 3.50 | 3.89 | 3/4 | | | ISG-ISCP |
| Transporter | | | | | | | | | | | | | |
| 51 | GTR1 | P11166 | *SLC2A1* | 4.31 | 4.13 | 0.70 | 2.56 | 1.99 | 2.74 | 3/5 | | | |
| 52 | TAP1 | Q03518 | *TAP1* | ND | 3.65 | ND | 2.90 | 2.74 | 3.10 | 3/3 | | | |
| Unknown | | | | | | | | | | | | | |
| 53 | EFHD2 | Q96C19 | *EFHD2* | 2.95 | ND | ND | 2.18 | 2.55 | 2.56 | 3/3 | | | |

[a] Proteins were classified using GO criteria according to biological function.

[b] Fold changes in target protein expression in tumor (T) and non-tumor (N) cells. Freq., frequency of target up- or down-regulated proteins in detectable samples; ND, not detected; NQ, detected but not quantified.

[c] Target proteins that were dysregulated in tumor cells as determined using genomics (G), proteomics (P), IHC, and Western blot (WB) approaches.

10 paired OSCC specimens by immunohistochemical staining (supplemental Fig. S2). The staining results were evaluated by two pathologists and scored as either negative, weak, moderate, or strong expression. The specificity of each antibody was verified by Western blot analysis using protein extracts from an oral cancer cell line (supplemental Fig. S3). A representative staining pattern for one paired tissue section (case 9) per protein as well as the scoring results for the 12 candidates are shown in Fig. 5, *B* and *C*, respectively. Comparison of staining scores from tumor and non-tumor counterparts revealed that, with the exception of ANAX3, 11 of the 12 candidates were significantly overexpressed (in more than eight of the 10 paired specimens) in tumor cells. The representative MS and MS/MS spectra used for the identification and quantification of these validated proteins are shown in supplemental Fig. S4. Collectively these observations demonstrate the consistency in results obtained from MS-based identification/quantification and our immunohistochemical validation. In addition, these results indicate the feasibility of using this technology platform to discover aberrantly expressed proteins in microdissected OSCC cells.

*MetaCore Analysis of Altered Signaling Pathways in OSCC*—To determine which biological networks are affected by the dysregulated proteins, the 80 MS-identified candidates were analyzed using MetaCore (version 4.7) (53). The analysis revealed six significantly altered pathways ($p < 0.001$) in OSCC lesions, including pathways related to keratin filament remodeling, IFN-$\alpha/\beta$ signaling, non-junctional endothelial cell contact, antiviral actions of IFNs, GPIb-IX-V-dependent platelet activation, and tetraspanin contributions to integrin-mediated cell adhesion (Table III). Data obtained for two prominent pathways (keratin filaments involved in cytoskeleton remodeling ($-\log_{p\ \mathrm{value}} = 19.364$) and type I IFN signaling ($-\log_{p\ \mathrm{value}} = 5.695$)) are shown in Fig. 6.

*Up-regulation of IFN-β-mediated Signaling Pathway in OSCC*—The results described above suggested that the type I IFN signaling pathway was significantly altered in OSCC lesions. We determined that 10 of the 53 up-regulated candidates were members of the IFN-stimulated gene (ISG) family (54–56), including SYWC, IFM1, STAT1, TYPH, UCRP, MX1, GBP1, GBP2, PML, and AMPL (Table I). Therefore, it is possible that an upstream regulator of this pathway (*e.g.* IFN-$\beta$) would be up-regulated in OSCC as well. This notion was confirmed by immunohistochemical staining, which clearly revealed the overexpression of IFN-$\beta$ in all 10 pairs of OSCC tissue sections (Fig. 7*A*). To explore the possible biological role of IFN-$\beta$ in OSCC, the effects of IFN-$\beta$ on cell proliferation and expression of two ISGs (UCRP and STAT1) were investigated in OSCC cells. Our results revealed that IFN-$\beta$ treatment for 1–3 days had a marginal effect (~10–20%) on the growth of OC3 cells (supplemental Fig. S5). In contrast, IFN-$\beta$ treatment significantly enhanced the expression of UCRP and STAT1 in OC3 cells (Fig. 7*B*), consistent with the prediction generated by GeneGo Map. The UCRP protein, also referred

TABLE II
*Down-regulated candidates in OSCC*

| GO[a] | Swiss-Prot | | Gene name | T/N ratio[b] | | | | | | | Cancer association[c] (detection method[c]) (Ref.) | | Possible regulation |
|---|---|---|---|---|---|---|---|---|---|---|---|---|---|
| | ID_HUMAN | Code | | 16N1 | 16T1 | 16T2 | 16N3 | 16T3 | Mean | Freq. | OSCC | Other cancers | |
| Cell organization and biogenesis | | | | | | | | | | | | | |
| 1 | K1C19 | P08727 | *KRT19* | 0.08 | 0.01 | 0.02 | 0.07 | 0.08 | 0.05 | 5/5 | | | |
| 2 | TSPO | P30536 | *TSPO* | 0.55 | 0.41 | ND | 0.24 | 0.31 | 0.38 | 3/4 | | | |
| Regulation of biological process | | | | | | | | | | | | | |
| 3 | HS70L | P34931 | *HSPA1L* | 0.44 | 0.30 | 0.54 | 0.22 | 0.24 | 0.35 | 4/5 | | | |
| 4 | HSP71 | P08107 | *HSPA1A* | 0.42 | 0.30 | 0.62 | 0.20 | 0.24 | 0.36 | 4/5 | | | ISCP |
| 5 | KCRU | P12532 | *CKMT1A* | 0.38 | 0.17 | ND | 0.35 | 0.46 | 0.34 | 4/4 | | | |
| 6 | AOFA | P21397 | *MAOA* | ND | 0.08 | ND | 0.08 | 0.17 | 0.11 | 3/3 | | | |
| Development | | | | | | | | | | | | | |
| 7 | K1C13 | P13646 | *KRT13* | 0.07 | 0.02 | 0.03 | 0.03 | 0.12 | 0.05 | 5/5 | (P, IHC) (17) | | |
| 8 | K1C15 | P19012 | *KRT15* | 0.08 | 0.03 | 0.07 | 0.01 | 0.12 | 0.06 | 5/5 | | Head and neck (139) | |
| 9 | PEPL | O60437 | *PPL* | 0.25 | 0.19 | 0.44 | 0.25 | 0.16 | 0.26 | 5/5 | | Head and neck (140) | |
| 10 | EVPL | Q92817 | *EVPL* | 0.31 | 0.24 | 0.39 | 0.25 | 0.19 | 0.28 | 5/5 | | | |
| 11 | SERA | O43175 | *PHGDH* | ND | 0.07 | ND | 0.05 | 0.14 | 0.09 | 3/3 | | | ISCP |
| 12 | PRELP | P51888 | *PRELP* | ND | 0.02 | 0.20 | NQ | ND | 0.11 | 2/2 | | | |
| Metabolism | | | | | | | | | | | | | |
| 13 | K2C4 | P19013 | *KRT4* | 0.04 | 0.05 | NQ | 0.03 | 0.13 | 0.06 | 4/4 | (P, IHC) (70) | Head and neck (15, 139) | |
| 14 | AL3A1 | P30838 | *ALDH3A1* | 0.10 | 0.09 | ND | 0.20 | 0.12 | 0.13 | 4/4 | | | |
| 15 | 6PGD | P52209 | *PGD* | 0.16 | 0.16 | 0.46 | 0.50 | ND | 0.32 | 3/4 | | | ISCP |
| 16 | AL4A1 | P30038 | *ALDH4A1* | 0.28 | ND | ND | 0.22 | 0.19 | 0.23 | 3/3 | | | |
| 17 | AL3A2 | P51648 | *ALDH3A2* | 0.19 | 0.15 | ND | 0.35 | NQ | 0.23 | 3/3 | | | |
| 18 | EST2 | O00748 | *CES2* | 0.39 | ND | 0.16 | 0.16 | ND | 0.24 | 3/3 | | | |
| 19 | TTL12 | Q14166 | *TTLL12* | 0.35 | 0.32 | ND | ND | 0.33 | 0.34 | 3/3 | | | |
| 20 | ADH7 | P40394 | *ADH7* | 0.005 | 0.02 | ND | ND | ND | 0.01 | 2/2 | | | |
| 21 | AL1A1 | P00352 | *ALDH1A1* | 0.002 | 0.06 | ND | ND | ND | 0.03 | 2/2 | | | |
| 22 | ALDH2 | P05091 | *ALDH2* | 0.12 | 0.11 | ND | ND | ND | 0.11 | 2/2 | | | |
| 23 | AL9A1 | P49189 | *ALDH9A1* | 0.11 | 0.23 | ND | ND | ND | 0.17 | 2/2 | | | |
| Unknown | | | | | | | | | | | | | |
| 24 | S10AG | Q96FQ6 | *S100A16* | 0.40 | 0.26 | 0.43 | 0.43 | 0.42 | 0.39 | 5/5 | | | |
| 25 | MGST2 | Q99735 | *MGST2* | 0.23 | ND | ND | 0.27 | 0.24 | 0.24 | 3/3 | | | |
| 26 | TACD2 | P09758 | *TACSTD2* | 0.36 | 0.28 | ND | ND | 0.25 | 0.30 | 3/3 | | | |
| 27 | S10AE | Q9HCY8 | *S100A14* | 0.30 | 0.23 | ND | 0.49 | ND | 0.34 | 3/3 | | Bladder (141), esophagus (142) | |

[a] Proteins were classified using GO criteria according to biological function.

[b] Fold changes in target protein expression in tumor (T) and non-tumor (N) cells. Freq., frequency of target up- or down-regulated proteins in detectable samples; ND, not detected; NQ, detected but not quantified.

[c] Target proteins that were dysregulated in tumor cells as determined using proteomics (P) and IHC approaches.

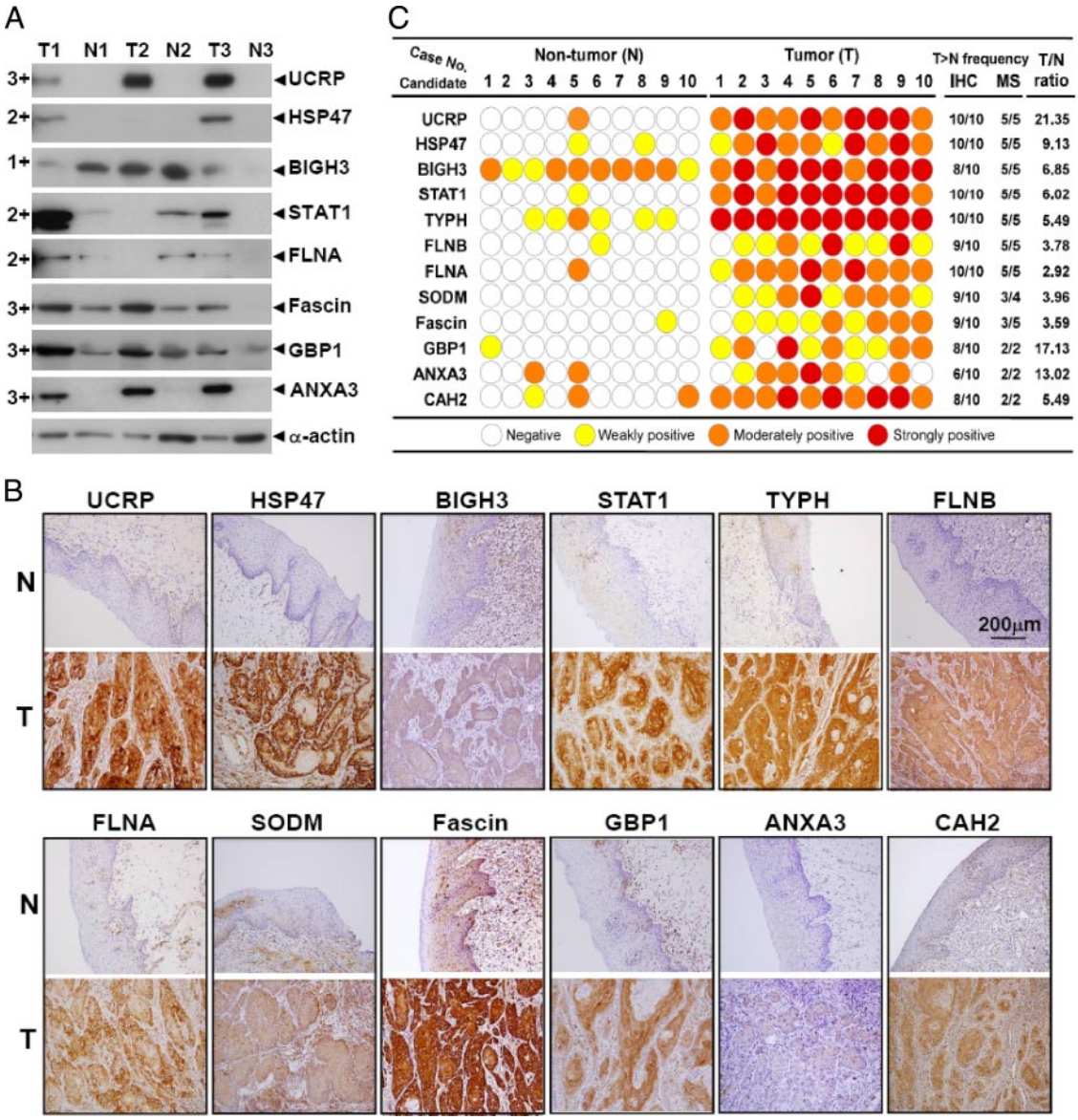


FIG. 5. **Confirmation of up-regulated proteins in OSCC tissue specimens by Western blot analysis and IHC staining.** *A*, Western blot analysis of eight up-regulated proteins in three paired tumor (*T*) and non-tumor (*N*) OSCC specimens. The actin signal was used as a loading control. The *3+*, *2+*, and *1+* designations indicate that the candidate proteins were overexpressed in three, two, and one sample, respectively. *B*, the IHC staining scores for 12 up-regulated candidates in 10 paired OSCC tissue sections. "*9/10*" indicates that the candidate was overexpressed (T > N) in nine of the 10 tumor epithelia tested. The T/N ratio and overexpression frequency (T > N) of the target candidates, as determined via MS-based analysis, are shown for comparison. *C*, representative IHC staining patterns for each validated candidate (*magnification*, 200×). *Scale bar*, 200 μm.

to as ISG15, is known to play a critical role in the IFN-mediated immune response against antiviral infection (57, 58). Through a mechanism called ISGylation, UCRP, like ubiquitin, conjugates with a variety of cellular proteins that modulate diverse cellular functions such as RNA processing, stress response, metabolism, cytoskeleton organization, and regulation (59, 60). We found that IFN-β treatment also stimulated UCRP expression in another OSCC cell line (SCC4) and significantly enhanced the conjugation of UCRP with cellular proteins (via ISGylation) (Fig. 7*C*). Notably ISGylation was concomitantly enhanced in three OSCC tumor tissues that overexpressed UCRP as compared with adjacent non-tumor controls (Fig. 7*C*). Finally the cell motility of OC3 oral cancer cells increased significantly in response to IFN-β treatment (Fig. 7*D*). Collectively these results demonstrate that the IFN-β-mediated signaling pathway was up-regulated in OSCC lesions studied and that IFN-β stimulates UCRP expression, ISGylation, and migration of OSCC cells.

*Tissue Microarray Analysis of UCRP Expression in Head-and-neck Cancer*—To analyze the UCRP expression in oral

TABLE III
*Biological networks in which the 80 differentially expressed proteins participate*

| GeneGo map | $-\log_{p\ value}$ | Features (Swiss-Prot ID) |
|---|---|---|
| 1. Cytoskeleton remodeling, keratin filaments | 19.364 | EPIPL, EVPL, PEPL, K2C4, K2C6A, K2C6E, K1C13, K1C14, K1C15, K1C16, K1C17, K1C19 |
| 2. Immune response, IFN-$\alpha/\beta$ signaling pathway | 5.695 | STAT1, UCRP/ISG15, PML |
| 3. Cell adhesion, endothelial cell contacts by non-junctional mechanisms | 5.265 | FINC, ITA6, ITB4, ACTN1 |
| 4. Immune response, antiviral actions of interferons | 4.151 | SYWC, STAT1, MX1, 2DRA, HB2G, HLAG |
| 5. Blood coagulation, GPIb-IV-V-dependent platelet activation | 3.286 | FLNA, FLNB, ACTN1, COCA1, FIBA, FIBB |
| 6. Cell adhesion, role of tetraspanins in the integrin-mediated cell adhesion | 3.087 | FINC, COCA1, ACTN1 |

cancer in more detail, a larger cohort comprising 49 paired OSCC specimens (17 buccal cancers, 18 tongue cancers, 10 gum cancers, three hard palate cancers, and one mouth floor cancer) was surveyed by immunohistochemical staining again. The results showed that 48 of 49 (98.0%) were negative and 44 of 49 (89.8%) were moderately or strongly positive for UCRP staining in adjacent normal and tumor parts, respectively (supplemental Table S4). As OSCC is a subtype of head-and-neck cancer, thus we further examined UCRP expression using a head-and-neck tissue microarray chip containing 60 head-and-neck squamous cell carcinoma tissues and three normal gingival tissues. As shown in Fig. 8, UCRP was not detected in normal gingival tissues; however, moderate to strong staining of UCRP was detected in nine of 12 tissue sections from patients with cheek cancer, nine of 15 tissue sections from patients with tongue cancer, and six of 18 tissue sections from patients with larynx cancer. In addition, all three tissue sections from patients with upper jaw cancer exhibited weak UCRP staining, whereas UCRP was not detected in tissue sections from patients with nose cancer. These results indicate that UCRP is highly expressed in OSCC lesions at different sites within the oral cavity.

## DISCUSSION

Laser capture microdissection is often used in conjunction with MS-based protein identification technology to assist with the discovery of tumor-associated molecules in tissue specimens containing various types of cells (27, 31, 61–64). However, relatively few studies have used these techniques to identify OSCC/HNSCC-associated proteins in tissue specimens from patients with OSCC/HNSCC (15, 17, 29). For example, Melle *et al.* (29) used ProteinChip technology and 2D gel electrophoresis to examine the up-regulation of annexin V in microdissected HNSCC tissues. In addition, Baker *et al.* (17) used LC-MS/MS to identify ~100 unique proteins in sets of normal and cancerous microdissected tongue specimens and used immunohistochemistry to demonstrate the down-regulation of cytokeratin (CK) 13 and the up-regulation of heat-shock protein 90 in tumor cells. Another recent study used LC-MS/MS to analyze the proteins extracted from microdissected formalin-fixed, paraffin-embedded tissue sections of normal oral epithelium as well as well, moderately, and poorly differentiated oral cancers. The authors identified 391 and 866 total proteins in the normal oral epithelia and in well differentiated oral cancer tumors, respectively (15). This study explored the relative distribution of identified proteins in tissue samples by counting the peptide numbers of each protein detected. In addition, the authors validated the expression of cytokeratins 4 and 16, desmoplakin, desmoglein 3, and vimentin proteins using immunohistochemistry (15). Although these studies identified and confirmed several OSCC/HNSCC-associated proteins, a more global view of the changes in protein expression in microdissected OSCC cells and adjacent non-tumor epithelial cells can be achieved using a precise quantification approach. Here we describe a quantitative technology platform that combines $^{18}O$ labeling, comprehensive 2D LC separation, and integrated ESI-MALDI MS/MS measurements. This technique was successfully used to identify and quantitate 977 proteins in microdissected samples from three pairs of freshly resected OSCC specimens. Among the MS-quantified proteins, we identified 53 up-regulated and 27 down-regulated proteins with fold changes $\geq$2.5. The reliability of the MS-based protein identification/quantification platform was confirmed via immunohistochemical validation experiments, which revealed that more than 90% of the 12 up-regulated proteins were overexpressed in OSCC tumor cells (Fig. 5 and supplemental Fig. S2). In addition, the reliability of this platform was confirmed by other immunohistochemical studies showing that five additional candidates (K1C16, TENA, FINC, TSP1, and NDRG1) were overexpressed in OSCC tissues (Table I). Finally 12 of the 53 up-regulated proteins (SYWC, K1C16, STAT1, TYPH, LDHA, K1C17, GRP78, SODM, ITB4, TPM4, K1C14, and GTR1) appeared to be overexpressed in OSCC tissues as determined by counting the peptides detected in microdissected OSCC samples from formalin-fixed, paraffin-embedded tissues sections (Table I and Ref. 15). To our knowledge, this is the largest quantitative proteomics data set of microdissected OSCC specimens reported to date.

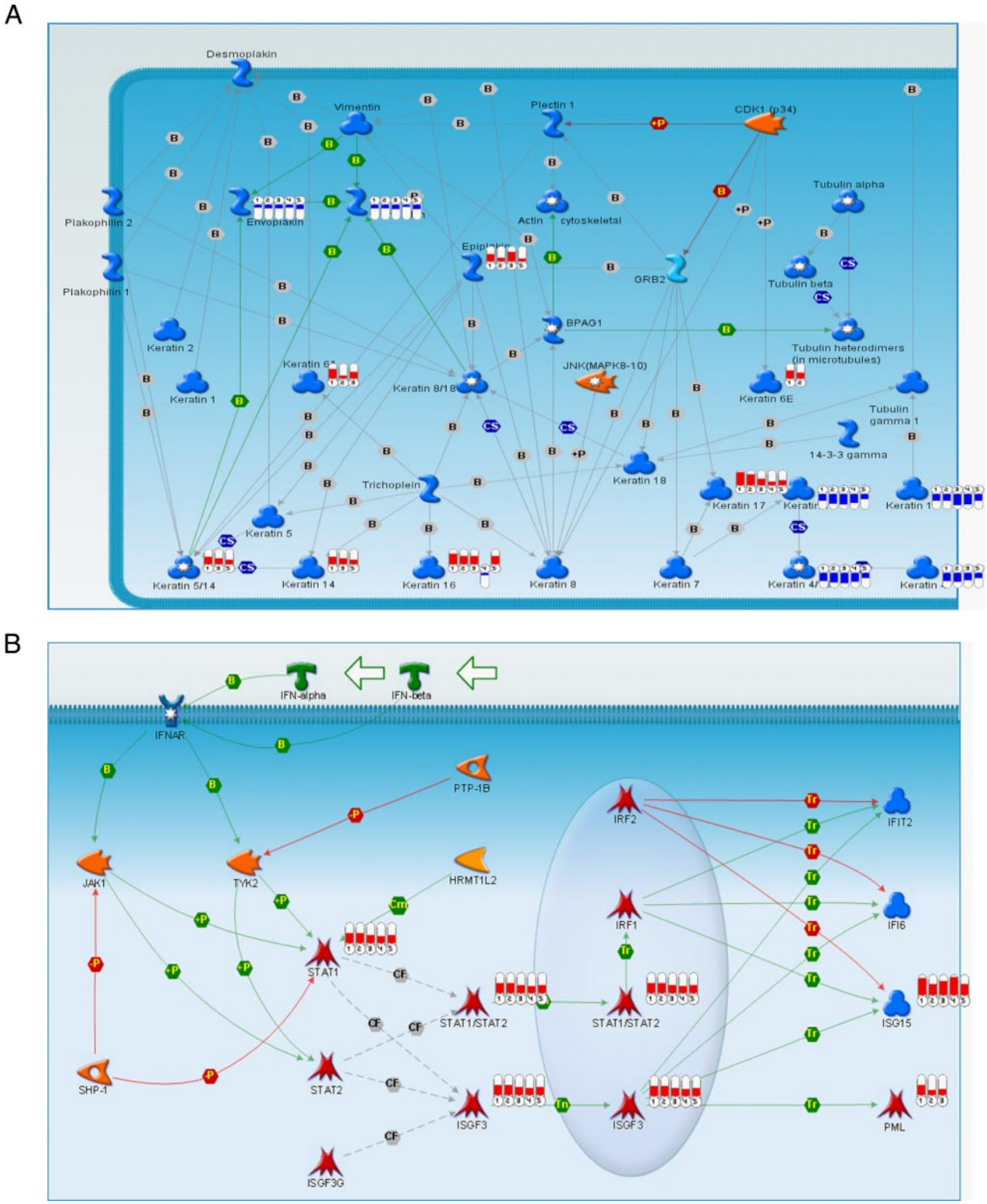


FIG. 6. **MetaCore analysis of altered signaling pathways in OSCC samples.** *A*, the cytoskeleton remodeling-keratin filaments pathway. *B*, the type I IFN signaling pathway. *Bars* labeled in *red* and *blue* denote up- and down-regulated target proteins, respectively. *Numbers* on the *bar* indicate the experiment in which the target was quantified. *1*, 16N1/18T1; *2*, 16N3/18T3; *3*, 16T1/18N1; *4*, 16T2/18N2; *5*, 16T3/18N3. *JNK*, c-Jun $NH_2$-terminal kinase; *MAPK*, mitogen-activated protein kinase; *IFNAR*, IFN-alpha/beta receptor. Interaction mechanism is marked with a symbol in the *hexagon* in the *middle* of the interaction arrow. *CF*, complex formation; *Cm*, covalent modifications; *Tr*, transcription regulation; *B*, binding; *+P*, phosphorylation; *−P*, dephosphorylation; *Tn*, transport; *CS*, complex subunit.

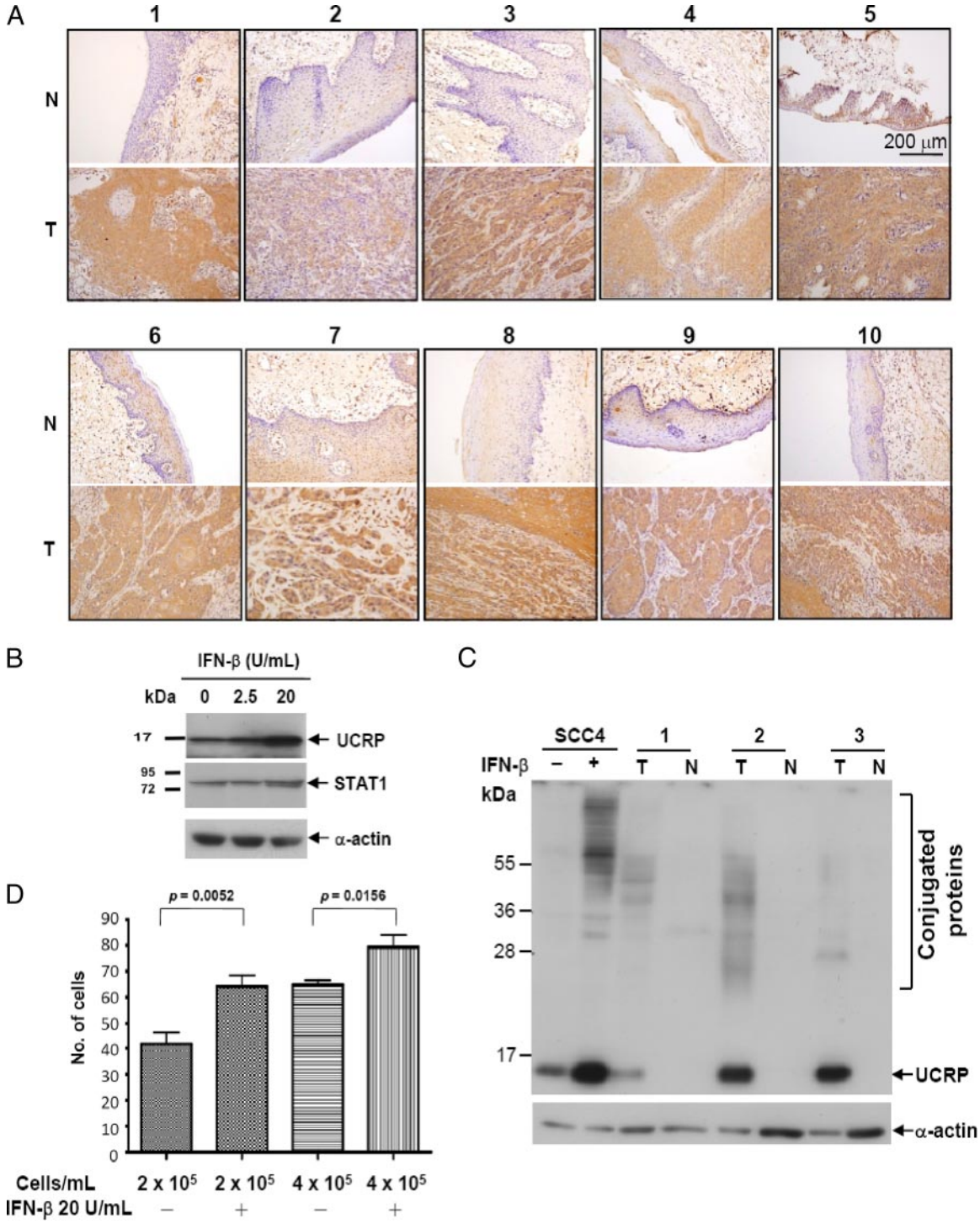


FIG. 7. **Alterations in the IFN signaling pathway.** *A*, IHC staining of IFN-β in 10 pairs of OSCC specimens. *B*, IFN-β stimulates the expression of UCRP and STAT1 in OC3 oral cancer cells. *C*, enhanced expression of UCRP and conjugated proteins in IFN-β-treated SCC4 cells and in three pairs of OSCC tissue specimens as detected by Western blotting. The α-actin signal was used as a loading control. *D*, IFN-β treatment enhanced the migration of OC3 cells in Transwell migration assays. The data correspond to mean values of cell number obtrained from six independent fields per well. *Error bars* denote the standard deviations.

At present, we cannot exclude the potential bias of our findings due to the inclusion of only male subjects in this study (16 patients; three for MS experiments, 10 for IHC staining, and three for Western blotting) (supplemental Table S1) and the small number of patients ($n = 3$) for the MS-based biomarker discovery. It is noted, however, that the majority of

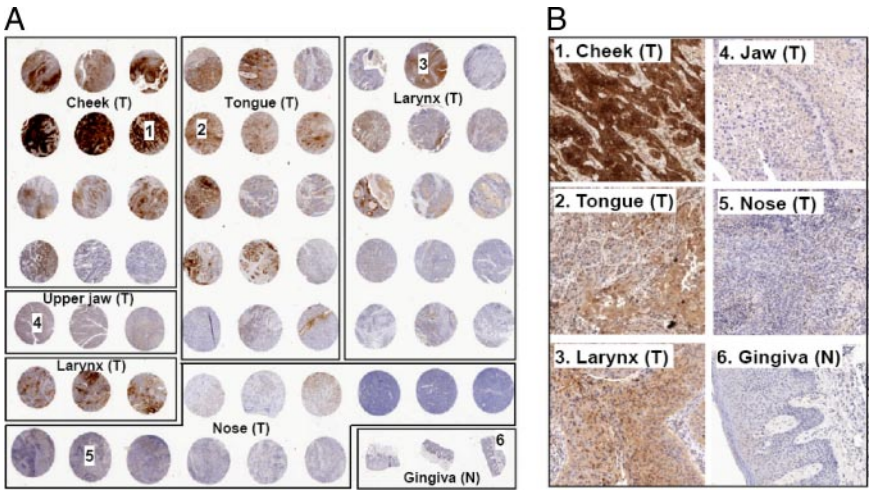


FIG. 8. **Tissue microarray analysis of UCRP/ISG15 in head-and-neck cancer.** *A*, IHC staining of UCRP/ISG15 using a head-and-neck tumor tissue microarray containing 60 tumor tissue sections (including 12 cheek, 15 tongue, 18 larynx, 12 nose, and three upper jaw tumors) and three normal gingival tissue sections. *B*, enlarged images of the stained sections shown in *A*.

oral cancer patients in Taiwan are male (85–93%) (65, 66). In addition, among the 53 up-regulated candidates identified from the three pairs of OSCC samples used here, more than 20 candidates have been confirmed and/or rediscovered to be overexpressed in OSCC tissues using a larger number of samples in the present study or by other groups (Ref. 15 and Table I and references cited therein). This observation indicates that, although potential bias may result from using specimens from a limited number of male patients, the quantitative proteome data set generated here can be useful for searching potential OSCC biomarkers.

Recently Siu and co-workers (16, 39) used an isobaric mass tag (iTRAQ (isobaric tags for relative and absolute quantitation)) labeling method and LC-MS/MS to identify several differentially expressed proteins in OSCC. The authors identified a total of 811 non-redundant proteins in tumor tissues and described a panel of proteins displaying consistently differential expression in tumors relative to non-cancerous controls. Several up-regulated candidates (*e.g.* FSCN1, LDHA, SODM, S10A2, and K1C14) were also identified in this study (Table I and Ref. 16). The authors also used immunohistochemistry analysis to identify a panel of up-regulated proteins (*e.g.* 14-3-3 $\sigma$ (stratifin), 14-3-3 $\zeta$, and calcium-binding protein S100A7) that could serve as potential markers for discriminating OSCC from non-cancerous tissues (16, 39). In our study, 14-3-3 $\sigma$ and 14-3-3 $\zeta$ (but not S100A7) were shown in five independent experiments to have T/N ratios ranging from 1.9 to 3.68 and from 1.33 to 3.14, respectively, in three of five experiments (supplemental Table S2). When a more stringent filter (T/N $\geq$2 in three of five experiments and an average ratio $\geq$2.5) was applied, these proteins were not included in our final candidate list. The differential protein expression patterns determined using different stable isotope labeling techniques were consistent, suggesting that stable isotope-dependent quantitative proteomics methods are reliable and feasible quantitative platforms.

Most (38 of 53) of the proteins that were up-regulated in tumor cells contributed to tumor-related biological processes such as cell proliferation, communication, defense, organization and biogenesis, and cell motility. The biological implications of these differentially expressed protein candidates were extracted using the MetaCore data mining suite. The most significant biological network identified in this analysis was the cytoskeleton remodeling-keratin filament pathway with a $-\log_{p\ \text{value}}$ of 19.364. The EPIPL and CK 6, 14, 16, and 17 proteins of this pathway were found to be up-regulated in oral cancer cells, whereas the EVPL, PEPL, and CK 4, 13, 15, and 19 proteins of this pathway were found to be down-regulated (Table III). Previous studies have shown that the transcription of CK6/16/17 can be induced in keratinocytes during wound healing (67, 68). In patients with OSCC, the loss of CK 13 or 19 expression may increase recurrence and enhance invasiveness (69). Although the molecular mechanisms of CK expression and regulation in tumor development remain unclear, the alterations in CK expression were consistent among different analytical platforms, highlighting the importance of keratin expression and regulation in oral cancer progression. A systematic investigation of keratin filament regulation may shed light on the development of epithelia and on the relative malignancy of tumor cells.

The second significant network identified in this study was the type I IFN signaling pathway ($-\log_{p\ \text{value}}$ of 5.695). Two key downstream regulators of this pathway (STAT1 and UCRP/ISG15) were identified and quantified in all five experiments with fold changes in expression in tumor and non-tumor cells ranging from 3.94 to 8.37 (STAT1) and 8.71 to 38.99 (UCRP/ISG15), respectively. Hundreds of ISG proteins have been previously determined using genomics and proteomics approaches (54, 55). Our current study showed that 10 of the 53 up-regulated candidate proteins belong to the ISG family (Table I), and increased mRNA or protein levels of seven proteins (SYWC, IFM1, STAT1, TYPH, UCRP, MX1, and GBP2) have been detected in OSCC via previous genomics or proteomics studies (9, 10, 70). Of these up-regulated ISG proteins, four (STAT1, UCRP, GBP1, and TYPH) were confirmed to be overexpressed in OSCC tissues via immunohis-

tochemical staining (in at least eight of the 10 tissue pairs examined) (Fig. 5*B*). Most notably, IFN-$\beta$ (the key upstream regulator of this pathway) was also confirmed to be overexpressed in the tumor cells of all OSCC tissue pairs (Fig. 7*A*). Although previous genomics and proteomics studies have confirmed the dysregulation of type I IFN signaling components in OSCC/HNSCC (9, 10, 70), it remains unclear whether the components of this pathway are systemically altered in OSCC/HNSCC and whether this pathway contributes to OSCC/HNSCC progression. Our use of quantitative proteomics approaches, biological network analyses, Western blot analyses, and immunohistochemistry analyses provides strong evidence that this pathway is significantly enhanced in OSCC tumor cells.

Interferons are categorized as two types (type I (IFN-$\alpha$ and IFN-$\beta$) and type II (IFN-$\gamma$)). These molecules are multifunctional cytokines that possess antiviral, antiproliferative, and immunomodulatory activities (71–73). Type I IFNs are known to inhibit the growth of a variety of cancer cells, and this inhibition can be mediated, at least in part, by the Jak-STAT-mediated cell death pathway (74, 75). However, other studies have shown that some cancer cells are resistant to IFN-$\alpha/\beta$-mediated antiproliferation, which may be attributed to the deregulation of the Jak-STAT, NF-$\kappa$B, and phosphatidylinositol 3-kinase/AKT pathways in these cells (76–78). In this study, we found that OSCC cells respond to IFN-$\beta$ by activating downstream target genes and increasing protein ISGylation but that these cells are resistant to IFN-$\beta$-mediated inhibition of cell growth (Fig. 7, *B* and *C*, and supplemental Fig. S5). Interestingly we also found that the migration ability of OSCC cells was enhanced after exposure to IFN-$\beta$ (Fig. 7*D*). Collectively these observations suggest that the overexpression of IFN-$\beta$ in OSCC tissues may have unexpected and profound effects on OSCC cells. This intriguing possibility warrants further investigation.

The TYPH protein is overexpressed in a wide variety of solid tumors. This protein can be induced by several cytokines, including IFNs, and contributes to angiogenesis (79, 80). In addition, STAT1 is a key regulator of the IFN signaling pathway and is known to be overexpressed in OSCC tissues (70, 81). UCRP/ISG15, a critical molecule in the IFN-mediated immune response against antiviral infection, was recently identified as a novel tumor marker candidate in bladder and breast cancers (82, 83). We show here that UCRP/ISG15 was highly expressed in OSCC lesions at different sites of the oral cavity (Figs. 7 and 8, supplemental Fig. S2, and supplemental Table S4). Previous studies have shown that UCRP/ISG15 interferes with the ubiquitin/proteasome pathway and alters the sensitivity of tumor cells to camptothecin, an antitumor drug. This interference presumably involves ISGylation, which modifies the functions of various cellular proteins (83–85). We detected increased levels of UCRP/ISG15 and its protein conjugates in IFN-$\beta$-stimulated OSCC cells as well as in three oral tumor tissues studied (Fig. 7*C*). Approximately 200 ISG15-conjugated proteins (ISCPs), which are known to participate in modulating diverse cell functions, have been identified in eukaryotic cells using a combination of double affinity purification and MS-based proteomics approaches (59, 60). In addition, we detected 16 differentially expressed ISCPs in OSCC tissues, including 13 up-regulated (SYWC, STAT1, FLNA, FLNB, MX1, GBP1, EPIPL, LDHA, ANXA3, HSP47, PML, ACTN1, and AMPL) and three down-regulated (HSP71, SERA, and 6PGD) proteins (Tables I and II). Collectively these findings raise the intriguing possibility that overexpressed IFN-$\beta$, UCRP/ISG15, and ISCPs might modify certain properties of OSCC cells, such as their sensitivity to chemotherapy. Further studies are needed to explore this possibility.

*Acknowledgments*—We thank Dr. Leroy F. Liu for kindly providing the ISG15 antibody as well as Dr. Jui-Hung Chang and Cha-Wei Hsu for assistance with protein function annotation and software development, respectively.

* This work was supported by Ministry of Education Grants EMRPD150231 and EMRPD170191 (to Chang Gung University) and Chang Gung Memorial Hospital Grants CMRPD160096, CTRP1001, and CMRPD160097.

S The on-line version of this article (available at http://www.mcponline.org) contains supplemental material.

§§ To whom correspondence may be addressed. Tel.: 886-3-2118800 (ext. 5971); Fax: 886-3-2118800 (ext. 3533); E-mail: kychien@mail.cgu.edu.tw.

¶¶ To whom correspondence may be addressed. Tel.: 886-3-2118800 (ext. 5171); Fax: 886-3-2118891; E-mail: yusong@mail.cgu.edu.tw.

REFERENCES

1. Scully, C., and Bagan, J. V. (2007) Recent advances in Oral Oncology. *Oral Oncol.* **43,** 107–115
2. Funk, G. F., Karnell, L. H., Robinson, R. A., Zhen, W. K., Trask, D. K., and Hoffman, H. T. (2002) Presentation, treatment, and outcome of oral cavity cancer: a National Cancer Data Base report. *Head Neck* **24,** 165–180
3. Koch, B. B., Karnell, L. H., Hoffman, H. T., Apostolakis, L. W., Robinson, R. A., Zhen, W., and Menck, H. R. (2000) National cancer database report on chondrosarcoma of the head and neck. *Head Neck* **22,** 408–425
4. Zhen, W., Karnell, L. H., Hoffman, H. T., Funk, G. F., Buatti, J. M., and Menck, H. R. (2004) The National Cancer Data Base report on squamous cell carcinoma of the base of tongue. *Head Neck* **26,** 660–674
5. Jensen, L. H., Osterlind, K., and Rytter, C. (2008) Randomized cross-over study of patient preference for oral or intravenous vinorelbine in combination with carboplatin in the treatment of advanced NSCLC. *Lung Cancer* **62,** 85–91
6. Liao, C. T., Chang, J. T., Wang, H. M., Ng, S. H., Hsueh, C., Lee, L. Y., Lin, C. H., Chen, I. H., Huang, S. F., Cheng, A. J., and Yen, T. C. (2008) Analysis of risk factors of predictive local tumor control in oral cavity cancer. *Ann. Surg. Oncol.* **15,** 915–922
7. Tsantoulis, P. K., Kastrinakis, N. G., Tourvas, A. D., Laskaris, G., and Gorgoulis, V. G. (2007) Advances in the biology of oral cancer. *Oral Oncol.* **43,** 523–534
8. Diaz, E. M., Jr., Holsinger, F. C., Zuniga, E. R., Roberts, D. B., and Sorensen, D. M. (2003) Squamous cell carcinoma of the buccal mucosa: one institution's experience with 119 previously untreated patients. *Head Neck* **25,** 267–273
9. Alevizos, I., Mahadevappa, M., Zhang, X., Ohyama, H., Kohno, Y., Posner, M., Gallagher, G. T., Varvares, M., Cohen, D., Kim, D., Kent, R., Donoff, R. B., Todd, R., Yung, C. M., Warrington, J. A., and Wong, D. T. (2001)

Oral cancer in vivo gene expression profiling assisted by laser capture microdissection and microarray analysis. *Oncogene* **20,** 6196–6204
10. Ye, H., Yu, T., Temam, S., Ziober, B. L., Wang, J., Schwartz, J. L., Mao, L., Wong, D. T., and Zhou, X. (2008) Transcriptomic dissection of tongue squamous cell carcinoma. *BMC Genomics* **9,** 69
11. de Moraes, R. V., Oliveira, D. T., Landman, G., de Carvalho, F., Caballero, O., Nonogaki, S., Nishimoto, I., and Kowalski, L. P. (2008) E-cadherin abnormalities resulting from CPG methylation promoter in metastatic and nonmetastatic oral cancer. *Head Neck* **30,** 85–92
12. Wong, D. T. (2006) Salivary diagnostics powered by nanotechnologies, proteomics and genomics. *J. Am. Dent. Assoc.* **137,** 313–321
13. Cheng, A. J., Chen, L. C., Chien, K. Y., Chen, Y. J., Chang, J. T., Wang, H. M., Liao, C. T., and Chen, I. H. (2005) Oral cancer plasma tumor marker identified with bead-based affinity-fractionated proteomic technology. *Clin. Chem.* **51,** 2236–2244
14. Xie, H., Onsongo, G., Popko, J., de Jong, E. P., Cao, J., Carlis, J. V., Griffin, R. J., Rhodus, N. L., and Griffin, T. J. (2008) Proteomics analysis of cells in whole saliva from oral cancer patients via value-added three-dimensional peptide fractionation and tandem mass spectrometry. *Mol. Cell. Proteomics* **7,** 486–498
15. Patel, V., Hood, B. L., Molinolo, A. A., Lee, N. H., Conrads, T. P., Braisted, J. C., Krizman, D. B., Veenstra, T. D., and Gutkind, J. S. (2008) Proteomic analysis of laser-captured paraffin-embedded tissues: a molecular portrait of head and neck cancer progression. *Clin. Cancer Res.* **14,** 1002–1014
16. Ralhan, R., Desouza, L. V., Matta, A., Chandra Tripathi, S., Ghanny, S., Datta Gupta, S., Bahadur, S., and Siu, K. W. (2008) Discovery and verification of head-and-neck cancer biomarkers by differential protein expression analysis using iTRAQ labeling, multidimensional liquid chromatography, and tandem mass spectrometry. *Mol. Cell. Proteomics* **7,** 1162–1173
17. Baker, H., Patel, V., Molinolo, A. A., Shillitoe, E. J., Ensley, J. F., Yoo, G. H., Meneses-García, A., Myers, J. N., El-Naggar, A. K., Gutkind, J. S., and Hancock, W. S. (2005) Proteome-wide analysis of head and neck squamous cell carcinomas using laser-capture microdissection and tandem mass spectrometry. *Oral Oncol.* **41,** 183–199
18. Wang, Z., Jiang, L., Huang, C., Li, Z., Chen, L., Gou, L., Chen, P., Tong, A., Tang, M., Gao, F., Shen, J., Zhang, Y., Bai, J., Zhou, M., Miao, D., and Chen, Q. (2008) Comparative proteomics approach to screening of potential diagnostic and therapeutic targets for oral squamous cell carcinoma. *Mol. Cell. Proteomics* **7,** 1639–1650
19. Staab, C. A., Ceder, R., Jägerbrink, T., Nilsson, J. A., Roberg, K., Jörnvall, H., Höög, J. O., and Grafström, R. C. (2007) Bioinformatics processing of protein and transcript profiles of normal and transformed cell lines indicates functional impairment of transcriptional regulators in buccal carcinoma. *J. Proteome Res.* **6,** 3705–3717
20. Mlynarek, A. M., Balys, R. L., Su, J., Hier, M. P., Black, M. J., and Alaoui-Jamali, M. A. (2007) A cell proteomic approach for the detection of secretable biomarkers of invasiveness in oral squamous cell carcinoma. *Arch. Otolaryngol. Head Neck Surg.* **133,** 910–918
21. Weng, L. P., Wu, C. C., Hsu, B. L., Chi, L. M., Liang, Y., Tseng, C. P., Hsieh, L. L., and Yu, J. S. (2008) Secretome-based identification of Mac-2 binding protein as a potential oral cancer marker involved in cell growth and motility. *J. Proteome Res.* **7,** 3765–3775
22. Ye, H., Wang, A., Lee, B. S., Yu, T., Sheng, S., Peng, T., Hu, S., Crowe, D. L., and Zhou, X. (2008) Proteomic based identification of manganese superoxide dismutase 2 (SOD2) as a metastasis marker for oral squamous cell carcinoma. *Cancer Genomics Proteomics* **5,** 85–94
23. Liu, T., Qian, W. J., Mottaz, H. M., Gritsenko, M. A., Norbeck, A. D., Moore, R. J., Purvine, S. O., Camp, D. G., 2nd, and Smith, R. D. (2006) Evaluation of multiprotein immunoaffinity subtraction for plasma proteomics and candidate biomarker discovery using mass spectrometry. *Mol. Cell. Proteomics* **5,** 2167–2174
24. Issaq, H. J., Xiao, Z., and Veenstra, T. D. (2007) Serum and plasma proteomics. *Chem. Rev.* **107,** 3601–3620
25. Zhang, H., Liu, A. Y., Loriaux, P., Wollscheid, B., Zhou, Y., Watts, J. D., and Aebersold, R. (2007) Mass spectrometric detection of tissue proteins in plasma. *Mol. Cell. Proteomics* **6,** 64–71
26. Zang, L., Palmer Toy, D., Hancock, W. S., Sgroi, D. C., and Karger, B. L. (2004) Proteomic analysis of ductal carcinoma of the breast using laser capture microdissection, LC-MS, and $^{16}O/^{18}O$ isotopic labeling. *J. Proteome Res.* **3,** 604–612
27. Hood, B. L., Darfler, M. M., Guiel, T. G., Furusato, B., Lucas, D. A., Ringeisen, B. R., Sesterhenn, I. A., Conrads, T. P., Veenstra, T. D., and Krizman, D. B. (2005) Proteomic analysis of formalin-fixed prostate cancer tissue. *Mol. Cell. Proteomics* **4,** 1741–1753
28. Craven, R. A., and Banks, R. E. (2001) Laser capture microdissection and proteomics: possibilities and limitation. *Proteomics* **1,** 1200–1204
29. Melle, C., Ernst, G., Schimmel, B., Bleul, A., Koscielny, S., Wiesner, A., Bogumil, R., Moller, U., Osterloh, D., Halbhuber, K. J., and von Eggeling, F. (2003) Biomarker discovery and identification in laser microdissected head and neck squamous cell carcinoma with ProteinChip technology, two-dimensional gel electrophoresis, tandem mass spectrometry, and immunohistochemistry. *Mol. Cell. Proteomics* **2,** 443–452
30. von Eggeling, F., Davies, H., Lomas, L., Fiedler, W., Junker, K., Claussen, U., and Ernst, G. (2000) Tissue-specific microdissection coupled with ProteinChip array technologies: applications in cancer research. *BioTechniques* **29,** 1066–1070
31. Melle, C., Ernst, G., Schimmel, B., Bleul, A., Koscielny, S., Wiesner, A., Bogumil, R., Möller, U., Osterloh, D., Halbhuber, K. J., and von Eggeling, F. (2004) A technical triade for proteomic identification and characterization of cancer biomarkers. *Cancer Res.* **64,** 4099–4104
32. Unwin, R. D., Pierce, A., Watson, R. B., Sternberg, D. W., and Whetton, A. D. (2005) Quantitative proteomic analysis using isobaric protein tags enables rapid comparison of changes in transcript and protein levels in transformed cells. *Mol. Cell. Proteomics* **4,** 924–935
33. Shiio, Y., and Aebersold, R. (2006) Quantitative proteome analysis using isotope-coded affinity tags and mass spectrometry. *Nat. Protoc.* **1,** 139–145
34. Ong, S. E., Blagoev, B., Kratchmarova, I., Kristensen, D. B., Steen, H., Pandey, A., and Mann, M. (2002) Stable isotope labeling by amino acids in cell culture, SILAC, as a simple and accurate approach to expression proteomics. *Mol. Cell. Proteomics* **1,** 376–386
35. Ong, S. E., and Mann, M. (2006) A practical recipe for stable isotope labeling by amino acids in cell culture (SILAC). *Nat. Protoc.* **1,** 2650–2660
36. Miyagi, M., and Rao, K. C. (2007) Proteolytic $^{18}O$-labeling strategies for quantitative proteomics. *Mass Spectrom. Rev.* **26,** 121–136
37. Stewart, I. I., Thomson, T., and Figeys, D. (2001) $^{18}O$ labeling: a tool for proteomics. *Rapid Commun. Mass Spectrom.* **15,** 2456–2465
38. Hajkova, D., Rao, K. C., and Miyagi, M. (2006) pH dependency of the carboxyl oxygen exchange reaction catalyzed by lysyl endopeptidase and trypsin. *J. Proteome Res.* **5,** 1667–1673
39. Matta, A., DeSouza, L. V., Shukla, N. K., Gupta, S. D., Ralhan, R., and Siu, K. W. (2008) Prognostic significance of head-and-neck cancer biomarkers previously discovered and identified using iTRAQ-labeling and multidimensional liquid chromatography-tandem mass spectrometry. *J. Proteome Res.* **7,** 2078–2087
40. Sudha, R., Kawachi, N., Du, P., Nieves, E., Belbin, T. J., Negassa, A., Angeletti, R. H., and Prystowsky, M. B. (2007) Global proteomic analysis distinguishes biologic differences in head and neck squamous carcinoma. *Lab. Investig.* **87,** 755–766
41. Lin, S. C., Liu, C. J., Chiu, C. P., Chang, S. M., Lu, S. Y., and Chen, Y. J. (2004) Establishment of OC3 oral carcinoma cell line and identification of NF-kappaB activation responses to areca nut extract. *J. Oral Pathol. Med.* **33,** 79–86
42. Yang, C. Y., and Meng, C. L. (1994) Regulation of PG synthase by EGF and PDGF in human oral, breast, stomach, and fibrosarcoma cancer cell lines. *J. Dent. Res.* **73,** 1404–1415
43. Wu, C. C., Chen, H. C., Chen, S. J., Liu, H. P., Hsieh, Y. Y., Yu, C. J., Tang, R., Hsieh, L. L., Yu, J. S., and Chang, Y. S. (2008) Identification of collapsin response mediator protein-2 as a potential marker of colorectal carcinoma by comparative analysis of cancer cell secretomes. *Proteomics* **8,** 316–332
44. Wu, C. C., Chien, K. Y., Tsang, N. M., Chang, K. P., Hao, S. P., Tsao, C. H., Chang, Y. S., and Yu, J. S. (2005) Cancer cell-secreted proteomes as a basis for searching potential tumor markers: nasopharyngeal carcinoma as a model. *Proteomics* **5,** 3173–3182
45. Chien, K. Y., Chang, Y. S., Yu, J. S., Fan, L. W., Lee, C. W., and Chi, L. M. (2006) Identification of a new in vivo phosphorylation site in the cytoplasmic carboxyl terminus of EBV-LMP1 by tandem mass spectrometry. *Biochem. Biophys. Res. Commun.* **348,** 47–55

46. Tse, K. P., Tsang, N. M., Chen, K. D., Li, H. P., Liang, Y., Hsueh, C., Chang, K. P., Yu, J. S., Hao, S. P., Hsieh, L. L., and Chang, Y. S. (2007) MCP-1 promoter polymorphism at 2518 is associated with metastasis of nasopharyngeal carcinoma after treatment. *Clin. Cancer Res.* **13,** 6320–6326
47. Yu, J. S., Chen, W. J., Ni, M. H., Chan, W. H., and Yang, S. D. (1998) Identification of the regulatory autophosphorylation site of autophosphorylation-dependent protein kinase (auto-kinase). Evidence that auto-kinase belongs to a member of the p21-activated kinase family. *Biochem. J.* **334,** 121–131
48. Yang, Y., Zhang, S., Howe, K., Wilson, D. B., Moser, F., Irwin, D., and Thannhauser, T. W. (2007) A comparison of nLC-ESI-MS/MS and nLC-MALDI-MS/MS for GeLC-based protein identification and iTRAQ-based shotgun quantitative proteomics. *J. Biomol. Tech.* **18,** 226–237
49. Hattan, S. J., and Parker, K. C. (2006) Methodology utilizing MS signal intensity and LC retention time for quantitative analysis and precursor ion selection in proteomic LC-MALDI analyses. *Anal. Chem.* **78,** 7986–7996
50. Chen, H. S., Rejtar, T., Andreev, V., Moskovets, E., and Karger, B. L. (2005) Enhanced characterization of complex proteomic samples using LC-MALDI MS/MS: exclusion of redundant peptides from MS/MS analysis in replicate runs. *Anal. Chem.* **77,** 7816–7825
51. Bantscheff, M., Dümpelfeld, B., and Kuster, B. (2004) Femtomole sensitivity post-digest $^{18}O$ labeling for relative quantification of differential protein complex composition. *Rapid Commun. Mass Spectrom.* **18,** 869–876
52. Heller, M., Mattou, H., Menzel, C., and Yao, X. (2003) Trypsin catalyzed $^{16}O$-to-$^{18}O$ exchange for comparative proteomics: tandem mass spectrometry comparison using MALDI-TOF, ESI-QTOF, and ESI-ion trap mass spectrometers. *J. Am. Soc. Mass Spectrom.* **14,** 704–718
53. Nikolsky, Y., Ekins, S., Nikolskaya, T., and Bugrim, A. (2005) A novel method for generation of signature networks as biomarkers from complex high throughput data. *Toxicol. Lett.* **158,** 20–29
54. Rakkola, R., Matikainen, S., and Nyman, T. A. (2005) Proteome characterization of human NK-92 cells identifies novel IFN-alpha and IL-15 target genes. *J. Proteome Res.* **4,** 75–82
55. Der, S. D., Zhou, A., Williams, B. R., and Silverman, R. H. (1998) Identification of genes differentially regulated by interferon alpha, beta, or gamma using oligonucleotide arrays. *Proc. Natl. Acad. Sci. U. S. A.* **95,** 15623–15628
56. Yao, Y., Kubota, T., Sato, K., Takeuchi, H., Kitai, R., and Matsukawa, S. (2005) Interferons upregulate thymidine phosphorylase expression via JAK-STAT-dependent transcriptional activation and mRNA stabilization in human glioblastoma cells. *J. Neurooncol.* **72,** 217–223
57. Andersen, J. B., and Hassel, B. A. (2006) The interferon regulated ubiquitin-like protein, ISG15, in tumorigenesis: friend or foe? *Cytokine Growth Factor Rev.* **17,** 411–421
58. Pitha-Rowe, I. F., and Pitha, P. M. (2007) Viral defense, carcinogenesis and ISG15: novel roles for an old ISG. *Cytokine Growth Factor Rev.* **18,** 409–417
59. Zhao, C., Denison, C., Huibregtse, J. M., Gygi, S., and Krug, R. M. (2005) Human ISG15 conjugation targets both IFN-induced and constitutively expressed proteins functioning in diverse cellular pathways. *Proc. Natl. Acad. Sci. U. S. A.* **102,** 10200–10205
60. Giannakopoulos, N. V., Luo, J. K., Papov, V., Zou, W., Lenschow, D. J., Jacobs, B. S., Borden, E. C., Li, J., Virgin, H. W., and Zhang, D. E. (2005) Proteomic identification of proteins conjugated to ISG15 in mouse and human cells. *Biochem. Biophys. Res. Commun.* **336,** 496–506
61. Cowherd, S. M., Espina, V. A., Petricoin, E. F., 3rd, and Liotta, L. A. (2004) Proteomic analysis of human breast cancer tissue with laser-capture microdissection and reverse-phase protein microarrays. *Clin. Breast Cancer* **5,** 385–392
62. Sanders, M. E., Dias, E. C., Xu, B. J., Mobley, J. A., Billheimer, D., Roder, H., Grigorieva, J., Dowsett, M., Arteaga, C. L., and Caprioli, R. M. (2008) Differentiating proteomic biomarkers in breast cancer by laser capture microdissection and MALDI MS. *J. Proteome Res.* **7,** 1500–1507
63. Gu, Y., Wu, S. L., Meyer, J. L., Hancock, W. S., Burg, L. J., Linder, J., Hanlon, D. W., and Karger, B. L. (2007) Proteomic analysis of high-grade dysplastic cervical cells obtained from ThinPrep slides using laser capture microdissection and mass spectrometry. *J. Proteome Res.* **6,** 4256–4268
64. Lu, Q., Murugesan, N., Macdonald, J. A., Wu, S. L., Pachter, J. S., and Hancock, W. S. (2008) Analysis of mouse brain microvascular endothelium using immuno-laser capture microdissection coupled to a hybrid linear ion trap with Fourier transform-mass spectrometry proteomics platform. *Electrophoresis* **29,** 2689–2695
65. Liao, C. T., Huang, S. F., Chen, I. H., Chang, J. T., Wang, H. M., Ng, S. H., Hsueh, C., Lee, L. Y., Lin, C. H., Cheng, A. J., and Yen, T. C. (2009) Risk stratification of patients with oral cavity squamous cell carcinoma and contralateral neck recurrence following radical surgery. *Ann. Surg. Oncol.* **16,** 159–170
66. Lo, W. L., Kao, S. Y., Chi, L. Y., Wong, Y. K., and Chang, R. C. (2003) Outcomes of oral squamous cell carcinoma in Taiwan after surgical therapy: factors affecting survival. *J. Oral Maxillofac. Surg.* **61,** 751–758
67. Paladini, R. D., Takahashi, K., Bravo, N. S., and Coulombe, P. A. (1996) Onset of re-epithelialization after skin injury correlates with a reorganization of keratin filaments in wound edge keratinocytes: defining a potential role for keratin 16. *J. Cell Biol.* **132,** 381–397
68. DePianto, D., and Coulombe, P. A. (2004) Intermediate filaments and tissue repair. *Exp. Cell Res.* **301,** 68–76
69. Crowe, D. L., Milo, G. E., and Shuler, C. F. (1999) Keratin 19 downregulation by oral squamous cell carcinoma lines increases invasive potential. *J. Dent. Res.* **78,** 1256–1263
70. Toruner, G. A., Ulger, C., Alkan, M., Galante, A. T., Rinaggio, J., Wilk, R., Tian, B., Soteropoulos, P., Hameed, M. R., Schwalb, M. N., and Dermody, J. J. (2004) Association between gene expression profile and tumor invasion in oral squamous cell carcinoma. *Cancer Genet. Cytogenet.* **154,** 27–35
71. Stark, G. R. (2007) How cells respond to interferons revisited: from early history to current complexity. *Cytokine Growth Factor Rev.* **18,** 419–423
72. Pfeffer, L. M., Dinarello, C. A., Herberman, R. B., Williams, B. R., Borden, E. C., Bordens, R., Walter, M. R., Nagabhushan, T. L., Trotta, P. P., and Pestka, S. (1998) Biological properties of recombinant alpha-interferons: 40th anniversary of the discovery of interferons. *Cancer Res.* **58,** 2489–2499
73. Takaoka, A., and Yanai, H. (2006) Interferon signalling network in innate defence. *Cell Microbiol.* **8,** 907–922
74. Kayagaki, N., Yamaguchi, N., Nakayama, M., Eto, H., Okumura, K., and Yagita, H. (1999) Type I interferons (IFNs) regulate tumor necrosis factor-related apoptosis-inducing ligand (TRAIL) expression on human T cells: A novel mechanism for the antitumor effects of type I IFNs. *J. Exp. Med.* **189,** 1451–1460
75. Choi, E. A., Lei, H., Maron, D. J., Wilson, J. M., Barsoum, J., Fraker, D. L., El-Deiry, W. S., and Spitz, F. R. (2003) Stat1-dependent induction of tumor necrosis factor-related apoptosis-inducing ligand and the cell-surface death signaling pathway by interferon beta in human cancer cells. *Cancer Res.* **63,** 5299–5307
76. Yang, C. H., Murti, A., Pfeffer, S. R., Kim, J. G., Donner, D. B., and Pfeffer, L. M. (2001) Interferon alpha/beta promotes cell survival by activating nuclear factor kappaB through phosphatidylinositol 3-kinase and Akt. *J. Biol. Chem.* **276,** 13756–13761
77. Yang, C. H., Murti, A., and Pfeffer, L. M. (1998) STAT3 complements defects in an interferon-resistant cell line: evidence for an essential role for STAT3 in interferon signaling and biological activities. *Proc. Natl. Acad. Sci. U. S. A.* **95,** 5568–5572
78. Lei, H., Furlong, P. J., Ra, J. H., Mullins, D., Cantor, R., Fraker, D. L., and Spitz, F. R. (2005) AKT activation and response to interferon-beta in human cancer cells. *Cancer Biol. Ther.* **4,** 709–715
79. Fukushima, M., Okabe, H., Takechi, T., Ichikawa, W., and Hirayama, R. (2002) Induction of thymidine phosphorylase by interferon and taxanes occurs only in human cancer cells with low thymidine phosphorylase activity. *Cancer Lett.* **187,** 103–110
80. Takebayashi, Y., Yamada, K., Ohmoto, Y., Sameshima, T., Miyadera, K., Yamada, Y., Akiyama, S., and Aikou, T. (1995) The correlation of thymidine phosphorylase activity with the expression of interleukin 1 alpha, interferon alpha and interferon gamma in human colorectal carcinoma. *Cancer Lett.* **95,** 57–62
81. Méndez, E., Fan, W., Choi, P., Agoff, S. N., Whipple, M., Farwell, D. G., Futran, N. D., Weymuller, E. A., Jr., Zhao, L. P., and Chen, C. (2007) Tumor-specific genetic expression profile of metastatic oral squamous cell carcinoma. *Head Neck* **29,** 803–814
82. Andersen, J. B., Aaboe, M., Borden, E. C., Goloubeva, O. G., Hassel, B. A.,

and Orntoft, T. F. (2006) Stage-associated overexpression of the ubiquitin-like protein, ISG15, in bladder cancer. *Br. J. Cancer* **94,** 1465–1471
83. Desai, S. D., Haas, A. L., Wood, L. M., Tsai, Y. C., Pestka, S., Rubin, E. H., Saleem, A., Nur-E-Kamal, A., and Liu, L. F. (2006) Elevated expression of ISG15 in tumor cells interferes with the ubiquitin/26S proteasome pathway. *Cancer Res.* **66,** 921–928
84. Desai, S. D., Wood, L. M., Tsai, Y. C., Hsieh, T. S., Marks, J. R., Scott, G. L., Giovanella, B. C., and Liu, L. F. (2008) ISG15 as a novel tumor biomarker for drug sensitivity. *Mol. Cancer Ther.* **7,** 1430–1439
85. Desai, S. D., Mao, Y., Sun, M., Li, T. K., Wu, J., and Liu, L. F. (2000) Ubiquitin, SUMO-1, and UCRP in camptothecin sensitivity and resistance. *Ann. N.Y. Acad. Sci.* **922,** 306–308
86. Ma, C., Rong, Y., Radiloff, D. R., Datto, M. B., Centeno, B., Bao, S., Cheng, A. W., Lin, F., Jiang, S., Yeatman, T. J., and Wang, X. F. (2008) Extracellular matrix protein betaig-h3/TGFBI promotes metastasis of colon cancer by enhancing cell extravasation. *Genes Dev.* **22,** 308–321
87. Buckhaults, P., Rago, C., St Croix, B., Romans, K. E., Saha, S., Zhang, L., Vogelstein, B., and Kinzler, K. W. (2001) Secreted and cell surface genes expressed in benign and malignant colorectal tumors. *Cancer Res.* **61,** 6996–7001
88. Schneider, D., Kleeff, J., Berberat, P. O., Zhu, Z., Korc, M., Friess, H., and Büchler, M. W. (2002) Induction and expression of betaig-h3 in pancreatic cancer cells. *Biochim. Biophys. Acta* **1588,** 1–6
89. Lee, T. K., Poon, R. T., Man, K., Guan, X. Y., Ma, S., Liu, X. B., Myers, J. N., and Yuen, A. P. (2007) Fascin over-expression is associated with aggressiveness of oral squamous cell carcinoma. *Cancer Lett.* **254,** 308–315
90. Chen, S. F., Yang, S. F., Li, J. W., Nieh, P. C., Lin, S. Y., Fu, E., Bai, C. Y., Jin, J. S., Lin, C. Y., and Nieh, S. (2007) Expression of fascin in oral and oropharyngeal squamous cell carcinomas has prognostic significance: a tissue microarray study of 129 cases. *Histopathology* **51,** 173–183
91. Hashimoto, Y., Ito, T., Inoue, H., Okumura, T., Tanaka, E., Tsunoda, S., Higashiyama, M., Watanabe, G., Imamura, M., and Shimada, Y. (2005) Prognostic significance of fascin overexpression in human esophageal squamous cell carcinoma. *Clin. Cancer Res.* **11,** 2597–2605
92. Zhang, H., Xu, L., Xiao, D., Xie, J., Zeng, H., Cai, W., Niu, Y., Yang, Z., Shen, Z., and Li, E. (2006) Fascin is a potential biomarker for early-stage oesophageal squamous cell carcinoma. *J. Clin. Pathol.* **59,** 958–964
93. Hashimoto, Y., Skacel, M., Lavery, I. C., Mukherjee, A. L., Casey, G., and Adams, J. C. (2006) Prognostic significance of fascin expression in advanced colorectal cancer: an immunohistochemical study of colorectal adenomas and adenocarcinomas. *BMC Cancer* **6,** 241
94. Jin, J. S., Yu, C. P., Sun, G. H., Lin, Y. F., Chiang, H., Chao, T. K., Tsai, W. C., and Sheu, L. F. (2006) Increasing expression of fascin in renal cell carcinoma associated with clinicopathological parameters of aggressiveness. *Histol. Histopathol.* **21,** 1287–1293
95. Yoder, B. J., Tso, E., Skacel, M., Pettay, J., Tarr, S., Budd, T., Tubbs, R. R., Adams, J. C., and Hicks, D. G. (2005) The expression of fascin, an actin-bundling motility protein, correlates with hormone receptor-negative breast cancer and a more aggressive clinical course. *Clin. Cancer Res.* **11,** 186–192
96. Pelosi, G., Pastorino, U., Pasini, F., Maissoneuve, P., Fraggetta, F., Iannucci, A., Sonzogni, A., De Manzoni, G., Terzi, A., Durante, E., Bresaola, E., Pezzella, F., and Viale, G. (2003) Independent prognostic value of fascin immunoreactivity in stage I nonsmall cell lung cancer. *Br. J. Cancer* **88,** 537–547
97. Hu, W., McCrea, P. D., Deavers, M., Kavanagh, J. J., Kudelka, A. P., and Verschraegen, C. F. (2000) Increased expression of fascin, motility associated protein, in cell cultures derived from ovarian cancer and in borderline and carcinomatous ovarian tumors. *Clin. Exp. Metastasis* **18,** 83–88
98. Dejmek, J. S., and Dejmek, A. (2006) The reactivity to CK5/6 antibody in tumor cells from non-small cell lung cancers shed into pleural effusions predicts survival. *Oncol. Rep.* **15,** 583–587
99. Ernst, M., Najdovska, M., Grail, D., Lundgren-May, T., Buchert, M., Tye, H., Matthews, V. B., Armes, J., Bhathal, P. S., Hughes, N. R., Marcusson, E. G., Karras, J. G., Na, S., Sedgwick, J. D., Hertzog, P. J., and Jenkins, B. J. (2008) STAT3 and STAT1 mediate IL-11-dependent and inflammation-associated gastric tumorigenesis in gp130 receptor mutant mice. *J. Clin. Investig.* **118,** 1727–1738
100. Ziober, A. F., Patel, K. R., Alawi, F., Gimotty, P., Weber, R. S., Feldman, M. M., Chalian, A. A., Weinstein, G. S., Hunt, J., and Ziober, B. L. (2006) Identification of a gene signature for rapid screening of oral squamous cell carcinoma. *Clin. Cancer Res.* **12,** 5960–5971
101. Yao, L., Itoh, S., and Furuta, I. (2002) Thymidine phosphorylase expression in oral squamous cell carcinoma. *Oral Oncol.* **38,** 584–590
102. Ranieri, G., Labriola, A., Achille, G., Florio, G., Zito, A. F., Grammatica, L., and Paradiso, A. (2002) Microvessel density, mast cell density and thymidine phosphorylase expression in oral squamous carcinoma. *Int. J. Oncol.* **21,** 1317–1323
103. Takao, S., Takebayashi, Y., Che, X., Shinchi, H., Natsugoe, S., Miyadera, K., Yamada, Y., Akiyama, S., and Aikou, T. (1998) Expression of thymidine phosphorylase is associated with a poor prognosis in patients with ductal adenocarcinoma of the pancreas. *Clin. Cancer Res.* **4,** 1619–1624
104. Ioachim, E. (2008) Thymidine phosphorylase expression in breast cancer: the prognostic significance and its association with other angiogenesis related proteins and extracellular matrix components. *Histol. Histopathol.* **23,** 187–196
105. Chen, L. C., Hsueh, C., Tsang, N. M., Liang, Y., Chang, K. P., Hao, S. P., Yu, J. S., and Chang, Y. S. (2008) Heterogeneous ribonucleoprotein k and thymidine phosphorylase are independent prognostic and therapeutic markers for nasopharyngeal carcinoma. *Clin. Cancer Res.* **14,** 3807–3813
106. Al-Adnani, M. S., Kirrane, J. A., and McGee, J. O. (1975) Inappropriate production of collagen and prolyl hydroxylase by human breast cancer cells in vivo. *Br. J. Cancer* **31,** 653–660
107. Matsui, H., Kubochi, K., Okazaki, I., Yoshino, K., Ishibiki, K., and Kitajima, M. (1999) Collagen biosynthesis in gastric cancer: immunohistochemical analysis of prolyl 4-hydroxylase. *J. Surg. Oncol.* **70,** 239–246
108. Yie, S. M., Yang, H., Ye, S. R., Li, K., Dong, D. D., and Lin, X. M. (2007) Expression of human leukocyte antigen G (HLA-G) correlates with poor prognosis in gastric carcinoma. *Ann. Surg. Oncol.* **14,** 2721–2729
109. Ramos, D. M., Chen, B., Regezi, J., Zardi, L., and Pytela, R. (1998) Tenascin-C matrix assembly in oral squamous cell carcinoma. *Int. J. Cancer* **75,** 680–687
110. Harada, T., Shinohara, M., Nakamura, S., and Oka, M. (1994) An immunohistochemical study of the extracellular matrix in oral squamous cell carcinoma and its association with invasive and metastatic potential. *Virchows Arch.* **424,** 257–266
111. Yoshikawa, K., Katagata, Y., and Kondo, S. (1998) Biochemical and immunohistochemical analyses of keratin expression in basal cell carcinoma. *J. Dermatol. Sci.* **17,** 15–23
112. Nikitakis, N. G., Rivera, H., Lopes, M. A., Siavash, H., Reynolds, M. A., Ord, R. A., and Sauk, J. J. (2003) Immunohistochemical expression of angiogenesis-related markers in oral squamous cell carcinomas with multiple metastatic lymph nodes. *Am. J. Clin. Pathol.* **119,** 574–586
113. Cao, D., Maitra, A., Saavedra, J. A., Klimstra, D. S., Adsay, N. V., and Hruban, R. H. (2005) Expression of novel markers of pancreatic ductal adenocarcinoma in pancreatic nonductal neoplasms: additional evidence of different genetic pathways. *Mod. Pathol.* **18,** 752–761
114. Maitra, A., Iacobuzio-Donahue, C., Rahman, A., Sohn, T. A., Argani, P., Meyer, R., Yeo, C. J., Cameron, J. L., Goggins, M., Kern, S. E., Ashfaq, R., Hruban, R. H., and Wilentz, R. E. (2002) Immunohistochemical validation of a novel epithelial and a novel stromal marker of pancreatic ductal adenocarcinoma identified by global expression microarrays: sea urchin fascin homolog and heat shock protein 47. *Am. J. Clin. Pathol.* **118,** 52–59
115. Yu, E., Lee, K. W., and Lee, H. J. (2000) Expression of promyelocytic leukaemia protein in thyroid neoplasms. *Histopathology* **37,** 302–308
116. Zheng, H. C., Takahashi, H., Li, X. H., Hara, T., Masuda, S., Guan, Y. F., and Takano, Y. (2008) Overexpression of GRP78 and GRP94 are markers for aggressive behavior and poor prognosis in gastric carcinomas. *Hum. Pathol.* **39,** 1042–1049
117. Langer, R., Feith, M., Siewert, J. R., Wester, H. J., and Hoefler, H. (2008) Expression and clinical significance of glucose regulated proteins GRP78 (BiP) and GRP94 (GP96) in human adenocarcinomas of the esophagus. *BMC Cancer* **8,** 70
118. Salzman, R., Kanková, K., Pácal, L., Tomandl, J., Horáková, Z., and Kostrica, R. (2007) Increased activity of superoxide dismutase in advanced stages of head and neck squamous cell carcinoma with locoregional metastases. *Neoplasma* **54,** 321–325

119. Hu, H., Luo, M. L., Du, X. L., Feng, Y. B., Zhang, Y., Shen, X. M., Xu, X., Cai, Y., Han, Y. L., and Wang, M. R. (2007) Up-regulated manganese superoxide dismutase expression increases apoptosis resistance in human esophageal squamous cell carcinomas. *Chin. Med. J.* **120,** 2092–2098
120. Ohuchida, K., Mizumoto, K., Miyasaka, Y., Yu, J., Cui, L., Yamaguchi, H., Toma, H., Takahata, S., Sato, N., Nagai, E., Yamaguchi, K., Tsuneyoshi, M., and Tanaka, M. (2007) Over-expression of S100A2 in pancreatic cancer correlates with progression and poor prognosis. *J. Pathol.* **213,** 275–282
121. Yao, R., Lopez-Beltran, A., Maclennan, G. T., Montironi, R., Eble, J. N., and Cheng, L. (2007) Expression of S100 protein family members in the pathogenesis of bladder tumors. *Anticancer Res.* **27,** 3051–3058
122. Kyriazanos, I. D., Tachibana, M., Dhar, D. K., Shibakita, M., Ono, T., Kohno, H., and Nagasue, N. (2002) Expression and prognostic significance of S100A2 protein in squamous cell carcinoma of the esophagus. *Oncol. Rep.* **9,** 503–510
123. Shinohara, M., Nakamura, S., Harada, T., Shimada, M., and Oka, M. (1996) Mode of tumor invasion in oral squamous cell carcinoma: improved grading based on immunohistochemical examination of extracellular matrices. *Head Neck* **18,** 153–159
124. Qi, Y., Chiu, J. F., Wang, L., Kwong, D. L., and He, Q. Y. (2005) Comparative proteomic analysis of esophageal squamous cell carcinoma. *Proteomics* **5,** 2960–2971
125. Ioachim, E., Charchanti, A., Briasoulis, E., Karavasilis, V., Tsanou, H., Arvanitis, D. L., Agnantis, N. J., and Pavlidis, N. (2002) Immunohistochemical expression of extracellular matrix components tenascin, fibronectin, collagen type IV and laminin in breast cancer: their prognostic value and role in tumour invasion and progression. *Eur. J. Cancer* **38,** 2362–2370
126. Warawdekar, U. M., Zingde, S. M., Iyer, K. S., Jagannath, P., Mehta, A. R., and Mehta, N. G. (2006) Elevated levels and fragmented nature of cellular fibronectin in the plasma of gastrointestinal and head and neck cancer patients. *Clin. Chim. Acta* **372,** 83–93
127. Pietruszewska, W., Kobos, J., Bojanowska-Poźniak, K., Durko, M., and Gryczyński, M. (2006) Immunohistochemical analysis of the fibronectin expression and its prognostic value in patients with laryngeal cancer. *Otolaryngol. Pol.* **60,** 697–702
128. Yao, L., Zhao, Y. L., Itoh, S., Wada, S., Yue, L., and Furuta, I. (2000) Thrombospondin-1 expression in oral squamous cell carcinomas: correlations with tumor vascularity, clinicopathological features and survival. *Oral Oncol.* **36,** 539–544
129. Hayashido, Y., Nakashima, M., Urabe, K., Yoshioka, H., Yoshioka, Y., Hamana, T., Kitano, H., Koizumi, K., and Okamoto, T. (2003) Role of stromal thrombospondin-1 in motility and proteolytic activity of oral squamous cell carcinoma cells. *Int. J. Mol. Med.* **12,** 447–452
130. Albo, D., and Tuszynski, G. P. (2004) Thrombospondin-1 up-regulates tumor cell invasion through the urokinase plasminogen activator receptor in head and neck cancer cells. *J. Surg. Res.* **120,** 21–26
131. Kodama, J., Hashimoto, I., Seki, N., Hongo, A., Yoshinouchi, M., Okuda, H., and Kudo, T. (2001) Thrombospondin-1 and -2 messenger RNA expression in invasive cervical cancer: correlation with angiogenesis and prognosis. *Clin. Cancer Res.* **7,** 2826–2831
132. Grossfeld, G. D., Carroll, P. R., Lindeman, N., Meng, M., Groshen, S., Feng, A. C., Hawes, D., and Cote, R. J. (2002) Thrombospondin-1 expression in patients with pathologic stage T3 prostate cancer undergoing radical prostatectomy: association with p53 alterations, tumor angiogenesis, and tumor progression. *Urology* **59,** 97–102
133. Miyanaga, K., Kato, Y., Nakamura, T., Matsumura, M., Amaya, H., Horiuchi, T., Chiba, Y., and Tanaka, K. (2002) Expression and role of thrombospondin-1 in colorectal cancer. *Anticancer Res.* **22,** 3941–3948
134. Albo, D., Shinohara, T., and Tuszynski, G. P. (2002) Up-regulation of matrix metalloproteinase 9 by thrombospondin 1 in gastric cancer. *J. Surg. Res.* **108,** 51–60
135. Chang, J. T., Wang, H. M., Chang, K. W., Chen, W. H., Wen, M. C., Hsu, Y. M., Yung, B. Y., Chen, I. H., Liao, C. T., Hsieh, L. L., and Cheng, A. J. (2005) Identification of differentially expressed genes in oral squamous cell carcinoma (OSCC): overexpression of NPM, CDK1 and NDRG1 and underexpression of CHES1. *Int. J. Cancer* **114,** 942–949
136. Yan, X., Chua, M. S., Sun, H., and So, S. (2008) N-Myc down-regulated gene 1 mediates proliferation, invasion, and apoptosis of hepatocellular carcinoma cells. *Cancer Lett*. **262,** 133–142
137. Chua, M. S., Sun, H., Cheung, S. T., Mason, V., Higgins, J., Ross, D. T., Fan, S. T., and So, S. (2007) Overexpression of NDRG1 is an indicator of poor prognosis in hepatocellular carcinoma. *Mod. Pathol.* **20,** 76–83
138. Wang, Z., Wang, F., Wang, W. Q., Gao, Q., Wei, W. L., Yang, Y., and Wang, G. Y. (2004) Correlation of N-myc downstream-regulated gene 1 overexpression with progressive growth of colorectal neoplasm. *World J. Gastroenterol.* **10,** 550–554
139. Chung, C. H., Parker, J. S., Karaca, G., Wu, J., Funkhouser, W. K., Moore, D., Butterfoss, D., Xiang, D., Zanation, A., Yin, X., Shockley, W. W., Weissler, M. C., Dressler, L. G., Shores, C. G., Yarbrough, W. G., and Perou, C. M. (2004) Molecular classification of head and neck squamous cell carcinomas using patterns of gene expression. *Cancer Cell* **5,** 489–500
140. Nishimori, T., Tomonaga, T., Matsushita, K., Oh-Ishi, M., Kodera, Y., Maeda, T., Nomura, F., Matsubara, H., Shimada, H., and Ochiai, T. (2006) Proteomic analysis of primary esophageal squamous cell carcinoma reveals downregulation of a cell adhesion protein, periplakin. *Proteomics* **6,** 1011–1018
141. Yao, R., Davidson, D. D., Lopez-Beltran, A., MacLennan, G. T., Montironi, R., and Cheng, L. (2007) The S100 proteins for screening and prognostic grading of bladder cancer. *Histol. Histopathol.* **22,** 1025–1032
142. Ji, J., Zhao, L., Wang, X., Zhou, C., Ding, F., Su, L., Zhang, C., Mao, X., Wu, M., and Liu, Z. (2004) Differential expression of S100 gene family in human esophageal squamous cell carcinoma. *J. Cancer Res. Clin. Oncol.* **130,** 480–486